Global and Planetary Change 208 (2022) 103680

Contents lists available at ScienceDirect

Global and Planetary Change

journal homepage: www.elsevier.com/locate/gloplacha

Research Paper

Impacts of marine heatwaves on tropical western and central Pacific Island nations and their communities

Neil J. Holbrook [a,b,*], Vanessa Hernaman [c], Shirley Koshiba [d], Jimaima Lako [e], Jules B. Kajtar [a,b], Patila Amosa [f], Awnesh Singh [g]

[a] Institute for Marine and Antarctic Studies, University of Tasmania, Hobart, Tasmania, Australia
[b] Australian Research Council Centre of Excellence for Climate Extremes, University of Tasmania, Hobart, Tasmania, Australia
[c] Climate Science Centre, CSIRO Oceans and Atmosphere, Aspendale, Victoria, Australia
[d] Palau International Coral Reef Center, Koror, Palau
[e] College of Engineering, Science and Technology, Fiji National University, Suva, Fiji
[f] Faculty of Science, The National University of Samoa, Apia, Samoa
[g] Pacific Centre for Environmental and Sustainable Development, The University of the South Pacific, Suva, Fiji

ARTICLE INFO

Editor: Howard Falcon-Lang

Keywords:
Marine heatwave
Extreme event
Impact
Ocean warming
Pacific
CMIP6 projections

ABSTRACT

Marine heatwaves can have devastating impacts on marine species and habitats, often with flow-on effects to human communities and livelihoods. This is of particular importance to Pacific Island countries that rely heavily on coastal and ocean resources, and for which projected increases in future marine heatwave (MHW) frequency, intensity, and duration could be detrimental across the Pacific Island region. In this study, we investigate MHWs in the tropical western and central Pacific Ocean region, focusing on observed MHWs, their associated impacts, and future projections using Coupled Model Intercomparison Project phase 6 (CMIP6) simulations under a low (SSP1–2.6) and a high (SSP5–8.5) greenhouse gas emissions scenario. Documented impacts from "Moderate" mean intensity MHW events in Fiji, Samoa, and Palau, that were categorised as "Strong" at their peak, included fish and invertebrate mortality and coral bleaching. Based on CMIP6 multi-model mean estimates, and relative to current baselines, "Moderate" intensity MHWs are projected to increase from recent historical (1995–2014) values of 10–50 days per year (dpy) across the region to the equivalent of >100 dpy by the year 2050 under the low emissions scenario, and > 200 dpy nearer the equator. Under the high emissions scenario, 200 dpy of Moderate MHW intensities are projected across most of the region by 2050, with >300 dpy nearer the equator. For the most intense "Extreme" category of MHW, estimates range from <1 dpy under the current climate to >50 dpy projected under the high emissions scenario by 2050. In contrast, "Extreme" MHWs are projected to increase to <5 dpy by 2050 under the low emissions scenario, highlighting the importance for Pacific Island nations that global emissions more closely follow the low emissions scenario trajectory.

1. Introduction

Pacific Island countries (PICs) comprise eight of 20 countries around the world with the highest annual average disaster losses, scaled by gross domestic product (The World Bank, 2013), making PICs among the most vulnerable in the world to natural hazards and climate change. The World Health Organization (WHO, 2015) identifies small island developing states (SIDS) – 20 of which are PICs – as particularly vulnerable to the health impacts of climate change, due to factors that include exposure to extreme climatic events. For example, marine fish food poisoning through ciguatera incidence has been linked to warmer sea surface temperatures that coincide with El Niño–Southern Oscillation (ENSO) cycles (Hales et al., 1999; Llewellyn, 2010; Skinner et al., 2011). Reports indicate that PICs have among the highest ciguatera rates in the world, and that these rates have increased in recent decades (Skinner et al., 2011). Climate change will also impact coastal and oceanic resources, upon which PIC communities are reliant in terms of food security, livelihoods, cultural heritage, and government revenue (Johnson et al., 2018, 2020).

Marine heatwaves (MHWs) – extreme and prolonged oceanic warm water events – can cause dramatic and sometimes devastating impacts to marine species and habitats (e.g. coral reefs, Hughes et al., 2018b; kelp,

* Corresponding author at: Institute for Marine and Antarctic Studies, University of Tasmania, Hobart, Tasmania, Australia.
E-mail address: neil.holbrook@utas.edu.au (N.J. Holbrook).

https://doi.org/10.1016/j.gloplacha.2021.103680
Received 14 October 2020; Received in revised form 13 July 2021; Accepted 13 October 2021
Available online 22 October 2021

Wernberg et al., 2013, 2016; Straub et al., 2019; Arafeh-Dalmau et al., 2020; seagrass, Arias-Ortiz et al., 2018; and ecosystems, Smale et al., 2019). Impacts of MHWs have been identified on fisheries and aquaculture (Mills et al., 2013; Oliver et al., 2017; Caputi et al., 2019; Cheung and Frölicher, 2020), with influences also on range shifts in fish species (Caputi et al., 2016; Pershing et al., 2018; Li et al., 2019; Yang et al., 2019). However, there are relatively limited reports that specifically link MHWs to impacts on coastal and offshore fisheries of Pacific Island countries (Nurse et al., 2014; IPCC, 2019). This is likely to be in large part due to our understanding of MHWs and their links to marine ecosystems and fisheries only being investigated over the past 10 years (e.g. Pearce et al., 2011; Mills et al., 2013; Pearce and Feng, 2013; Wernberg et al., 2013; Holbrook et al., 2019, 2020b; Smale et al., 2019).

Climate variability plays an important role in modulating MHWs (e.g. Di Lorenzo and Mantua, 2016; Scannell et al., 2016; Oliver et al., 2018) and their likelihoods (Holbrook et al., 2019), with ENSO clearly evident in signatures of MHW interannual variability (Oliver et al., 2018) and with significant impacts on shallow-water coastal marine ecosystems (e.g. Hughes et al., 2018a; Holbrook et al., 2020a). Given that the centre-of-action of ENSO is in the tropical Pacific (McPhaden et al., 2006) and plays a dominant role in influencing MHW likelihoods across the Pacific region (Holbrook et al., 2019), we expect that MHW occurrence likelihoods may be potentially predictable several months in advance in regions of the tropical Pacific (Holbrook et al., 2019, 2020b). Importantly, recent research suggests that climate predictions can potentially improve the sustainability of coastal fisheries in Pacific SIDS (Dunstan et al., 2018), with improved understanding of MHW predictability across the region being an important factor in that endeavour.

This paper examines observed MHWs and climate change projections of MHW metrics (frequency, intensity and duration) in the tropical western and central Pacific Ocean region (TWCPO; Fig. 1), together with case studies of observed impacts to marine ecosystems and fisheries of Pacific Island countries and their human communities. The paper focuses on the three Pacific Island nations of Fiji, Samoa and Palau as case study regions impacted by specific MHW events. More broadly, we consider the role of climate variability on MHW occurrences, the potential predictability of MHWs, and climate change projections on changes in MHW frequency, intensity and duration under both low and high carbon emissions scenarios. Previous analyses of climate change projections, based on the CMIP5 suite of climate models, show that MHWs are expected to increase in frequency, intensity and duration globally (Frölicher et al., 2018; Oliver et al., 2019). Here we investigate climate change projections based on the most recent CMIP6 suite of model simulations and focus our attention on the TWCPO. Recent research indicates that CMIP6 models perform slightly better than those in CMIP5 with respect to model biases in MHW metrics (Grose et al., 2020), thus making them possibly better suited for this regional study of the TWCPO.

The structure of the paper is outlined as follows. Section 2 describes the materials and methods employed in the study. Section 3 analyses historical MHW trends across the TWCPO. Specific MHW events and impacts are more closely examined in section 4 for the three PICs of Fiji, Samoa, and Palau. Future projections from a subset of CMIP6 climate models are outlined in section 5, and finally we provide an overall discussion in section 6.

2. Materials and methods

2.1. Observational sea surface temperature data

Sea surface temperature (SST) data primarily analysed in this study are from the U.S. National Oceanic and Atmospheric Administration (NOAA) ¼° daily Optimum Interpolation Sea Surface Temperature v2–1 dataset (hereafter called the daily OISST; Reynolds et al., 2007; Huang et al., 2021). These daily OISST represent a combination of observations from different platforms (satellites, ships, buoys, and Argo floats) on a regular ¼° global grid, interpolated to fill the gaps. As an evaluation of these data for use at scales relevant to this study – which include case study regions for the countries of Fiji, Samoa, and Palau – we analysed the daily OISST data against local in-situ observations of seawater temperatures. Data were available from http://www.reeftemps.science/en/data/ (Varillon et al., 2021) for 10 locations on Fijian reefs (depths of 9.5–16.2 m) between 2012 and 2019, and one in Samoa (4 m depth) from late-2012 to mid-2015 (Fig. 2a,b). For Palau, the International Coral Reef Center provided seawater temperature data from 11 data loggers deployed on Palau reefs from 2014 to 2019 (Fig. 2c).

We compared daily OISST with local data for this total of 22 locations, but only show representative sites here (Fig. 2). We found that intra- and inter-annual SST patterns observed on the reefs were well represented by the daily OISST data, as were local episodes of elevated SSTs (Fig. 2). The magnitudes of warming are also reflected very well in the daily OISST data, with exceptions only in five within-bay protected reefs in Palau, which all experienced 1–2 °C higher daily mean seawater temperatures than indicated by the OISST gridded data (e.g., Nikko3 in Fig. 2c). This is unsurprising given their sheltered within-bay position.

In summary, comparisons between local in-situ observations and the OISST data for all three country locations confirmed that the patterns and magnitudes of warming are generally represented very well by the daily OISST data. Hence, we consider this blended gridded product serves as a good proxy for local SSTs, and confirms the validity of using the gridded data to investigate MHWs and their variability across the TWCPO, as well as their characteristics and potential impacts more locally on the PICs of Fiji, Samoa, and Palau (Fig. 2).

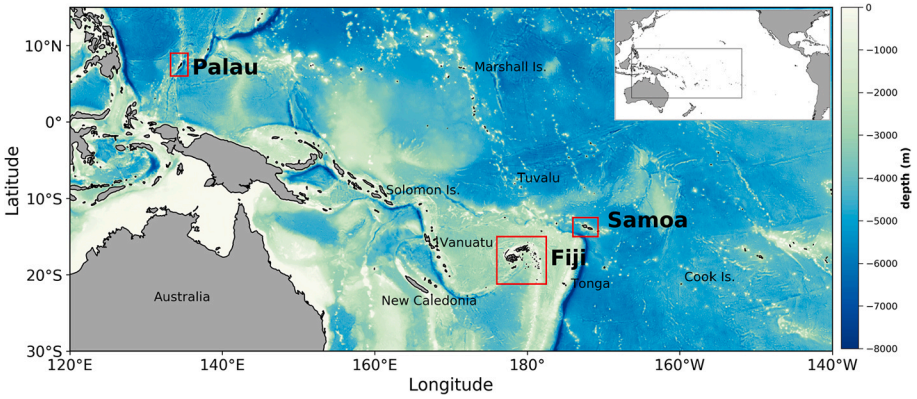

Fig. 1. Domain of the tropical western and central Pacific Ocean (TWCPO) region considered for the historical and projected MHW statistics, and the domains (red boxes) for each of the country-specific analyses for Palau, Fiji, and Samoa. Inset shows the TWCPO domain (black box) in the context of the wider Pacific. (For interpretation of the references to colour in this figure legend, the reader is referred to the web version of this article.)

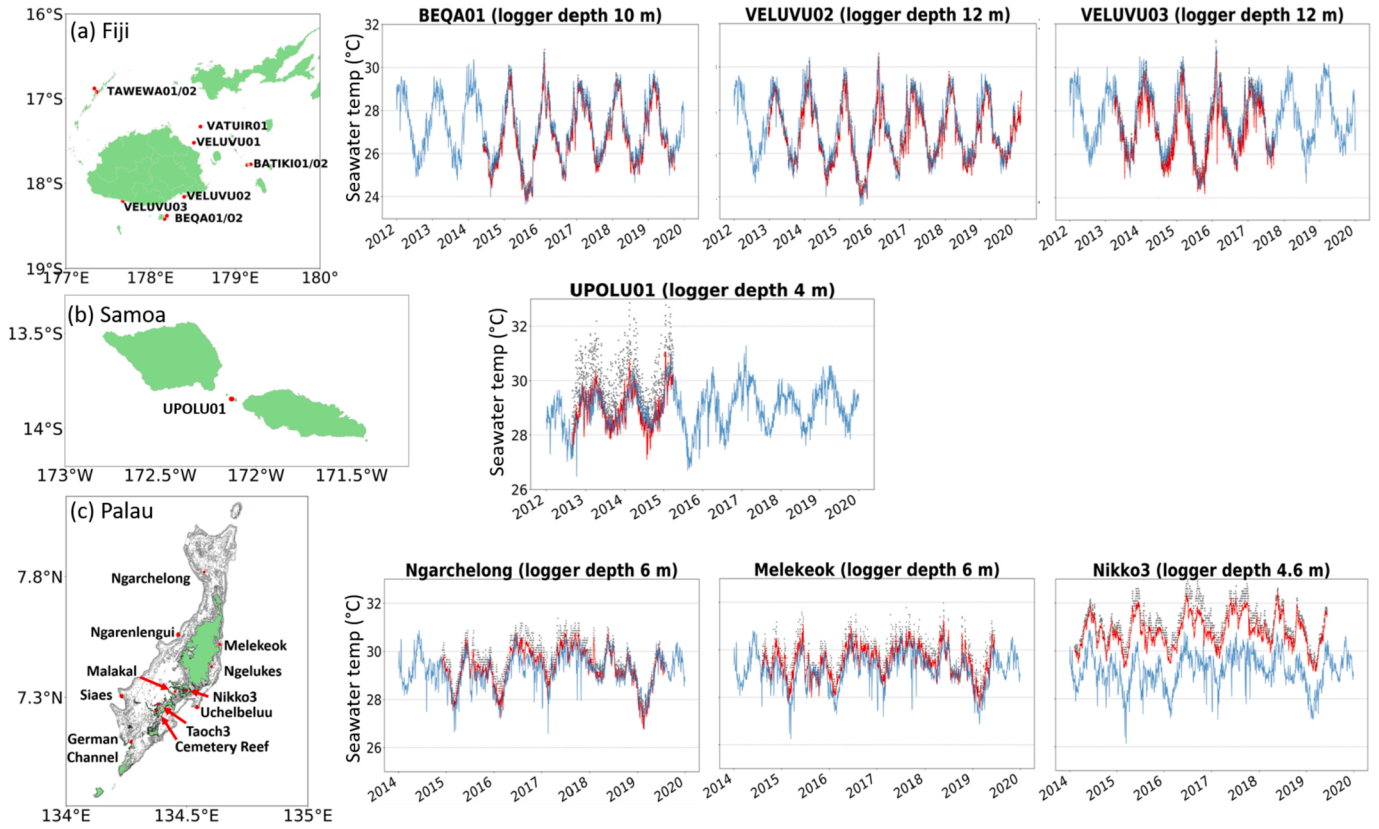

Fig. 2. Location of reef data loggers, and comparison of daily mean SST from the data logger (red line) with daily mean OISST data (blue line) extracted at the logger location. Also shown are the daily maximum temperatures recorded by the logger (grey dots). A total of 22 sites were evaluated, but only representative locations are shown here. (For interpretation of the references to colour in this figure legend, the reader is referred to the web version of this article.)

2.2. Characterisation of marine heatwaves

MHW metrics (frequency, intensity and duration) in space and time across the TWCPO were calculated from the daily OISST data. Here we used the Hobday et al. (2016, 2018) definitions of MHW events and their intensities (characterised by categories from I-IV; see below), where a MHW event is defined as a "discrete, prolonged anomalously warm water event" which lasts for five or more days, with temperatures warmer than the 90th percentile relative to climatological values. The 90th percentile threshold was uniquely computed for each calendar day and grid-point as follows. To increase the number of sample points, the threshold was computed over an 11-day window centred on the given day, sampling each year within the selected climatological period. After computing the threshold for each calendar day, the year-long timeseries was finally smoothed by applying a 31-day moving mean. The climatological mean was computed in a similar manner. MHW events were defined by their duration (number of days above the 90th percentile threshold), maximum intensity (maximum temperature above the climatological mean attained during the event), mean intensity, and cumulative intensity (sum (integral) of the daily intensities through the life-time of the MHW event occurrence; Hobday et al., 2016). We used a 30-year baseline (1986–2015) for the climatological mean and MHW threshold in Section 4, as recommended by Hobday et al. (2016), which is appropriate for examining MHWs in the observational record. A 20-year baseline (1995–2014) was used in Sections 3 and 5, which corresponds with Intergovernmental Panel on Climate Change (IPCC) Sixth Assessment Report (AR6) recommendations appropriate for projected changes relative to the historical period. Differences as a result of using these two baseline periods are minimal.

MHW categories are defined by multiples of the 90th percentile threshold. That is, the intensity category of a particular MHW at any point in time is identified by the temperature extreme category band within which the local difference between the observed SST and the seasonal climatology occurs, and includes "Moderate" (Category I, 1–2×), "Strong" (Category II, 2-3×), "Severe" (Category III, 3–4×), and "Extreme" (Category IV, >4×) (Hobday et al., 2018).

For each country, MHW events were investigated at the individual ¼° grid scale within each domain for specific MHW events, and also based on area-averaged timeseries within a domain over the observed record period (1982–2019).

2.3. Model data

We also examined MHW projections based on model outputs from those participating in the Coupled Model Intercomparison Project, phase 6 (CMIP6) – that is, the current generation of global climate simulations that will inform the 6th Assessment Report of the Intergovernmental Panel on Climate Change (IPCC AR6). Daily SST fields (variable name: tos) were analysed from the *historical* set of experiments, together with two future shared socioeconomic pathways (SSP) from the Scenario Model Intercomparison Project (ScenarioMIP; O'Neill et al., 2016): *SSP1–2.6* and *SSP5–8.5*. The historical experiments conclude at the end of year 2014, at which point the future scenarios are appended. A 20-year baseline (1995–2014) was used for the CMIP6 analysis. One ensemble member from each model and for each experiment was analysed. The requirement of having daily SST from each of the three experiments resulted in a set of 18 models with available data at the time of initial analysis (May 2020; Table 1).

The future scenarios selected for analysis are both 'Tier 1', indicating that they represent those being utilised by most modelling groups participating in the AR6 process. SSP1–2.6 is a low emissions pathway, following a 'sustainable' socio-economic future and resulting in 2.6 W/

Table 1
List of CMIP6 model data analysed in this study, along with their atmospheric and oceanic grid resolutions. For a given model, ensemble members with the same experiment identifiers were used across each of the three experiments. This does not guarantee that the future scenarios are branched from the same common historical experiment, but any differences are expected to have little impact on the results shown herein.

	Institute	Model	Experiment	Atmos. grid (lon × lat)	Ocean grid (lon × lat)
1	BCC	BCC-CSM2-MR	r1i1p1f1	320 × 160	360 × 232
2	CCCma	CanESM5	r1i1p1f1	128 × 64	361 × 290
3	CNRM-CERFACS	CNRM-CM6–1	r2i1p1f2	~192 × 128	362 × 294
4	CNRM-CERFACS	CNRM-CM6–1-HR	r1i1p1f2	~505 × 360	1442 × 1050
5	CNRM-CERFACS	CNRM-ESM2–1	r1i1p1f2	~192 × 128	362 × 294
6	CSIRO	ACCESS-ESM1–5	r1i1p1f1	192 × 145	360 × 300
7	CSIRO-ARCCSS	ACCESS-CM2	r1i1p1f1	192 × 144	360 × 300
8	EC-Earth-Consortium	EC-Earth3	r11i1p1f1	512 × 256	362 × 292
9	EC-Earth-Consortium	EC-Earth3-Veg	r1i1p1f1	512 × 256	362 × 292
10	IPSL	IPSL-CM6A-LR	r1i1p1f1	144 × 143	362 × 332
11	MIROC	MIROC6	r1i1p1f1	256 × 128	360 × 256
12	MOHC	HadGEM3-GC31-LL	r1i1p1f3	192 × 144	360 × 330
13	MOHC	UKESM1–0-LL	r1i1p1f2	192 × 144	360 × 330
14	MPI-M	MPI-ESM1–2-LR	r1i1p1f1	192 × 96	256 × 220
15	MRI	MRI-ESM2–0	r1i1p1f1	320 × 160	360 × 364
16	NCAR	CESM2	r4i1p1f1	288 × 192	320 × 384
17	NCC	NorESM2-LM	r1i1p1f1	144 × 96	360 × 384
18	NCC	NorESM2-MM	r1i1p1f1	288 × 192	360 × 384

m^2 of effective radiative forcing from greenhouse gases at year 2100. SSP5–8.5 is a high emissions scenario, with heavy future fossil-fuel development, and 8.5 W/m^2 of effective radiative forcing at year 2100. The exact emissions pathway that the planet will follow over the 21st century is highly uncertain, but there are reasonable expectations that it will be somewhere between these two scenarios. The approach adopted here to analyse results from climate change projections under both a low and high emissions scenario follows that of the recent IPCC Special Report on the Ocean and Cryosphere in a Changing Climate (SROCC; IPCC, 2019).

The CMIP6 MHW statistics were computed on a grid-point basis, using model data on native grids (using only '*gn*' data). For model aggregation, the computed MHW statistics were only re-gridded to the observed data grid in the final instance using nearest neighbour interpolation. This procedure ensures that temperature smoothing is avoided, which may have otherwise occurred if the data were re-gridded in the first instance using bilinear interpolation. For the regional case study analysis (Section 5.3), the model SST data were first area-averaged over each respective region before computing the marine heatwave statistics. Only data from the respective native grids that fell within the selected case study regions contributed to the area average. No regional downscaling was applied.

There are many caveats and limitations to working with projections from CMIP6 model data. Firstly, the set of 18 models analysed here represents a small number of the eventual total expected. Over 130 models have registered their source identifiers for CMIP6 with the World Climate Research Programme (WCRP; https://wcrp-cmip.github.io/CMIP6_CVs/), so the output from many more simulations may be available in the future. Further limitations arise from coarseness of model resolutions and individual model biases, among a host of other considerations (e.g. Fiedler et al., 2021). Aside from such limitations, other approaches may have been taken in analysing projections. For example, the CMIP5 suite of models could have been analysed together with CMIP6. However, different generations of models may also have different sets of biases (Grose et al., 2020; Zelinka et al., 2020). Regional climate simulations or regional downscaling (e.g. Hewitson et al., 2014; Giorgi and Gutowski Jr, 2015; Zhang et al., 2020) can be advantageous, although resource intensive. Another approach might be to work with auto-regressive modelled data, based on observed statistical properties (e.g. Holbrook et al., 2019; Oliver, 2019), with the incorporation of a shifting baseline, or other parameters, to simulate the effect of global warming (e.g. Ballester et al., 2009; Simolo et al., 2011; Oliver et al., 2014). Such an approach can be informative, but does not capture any dynamics, feedbacks or non-linearities. Given the wide range of considerations, we elected to analyse the available CMIP6 model data, that is, outputs from the latest generation of global climate models that have been utilised to inform IPCC AR6.

3. TWCPO marine heatwave characteristics and changes

3.1. Mean marine heatwave metrics

The tropical western and central Pacific Ocean (TWCPO) is a region subjected to substantial climate variability. The dominant mode of year-to-year (interannual) climate variability in this region, and globally, is El Niño–Southern Oscillation (ENSO), which has its centre-of-action in the tropical Pacific Ocean (e.g. McPhaden et al., 2006, 2020). El Niño and its opposite phase of La Niña are characterised by horseshoe patterns in SST anomalies across the Pacific Ocean. As a result, the TWCPO experiences a dipole-like climate pattern: when strong SST anomalies emerge along the central to eastern equatorial Pacific, anomalies of the opposite sign are evident to the south, north and west. Unsurprisingly, ENSO is the dominant driver of MHWs in this region, with stronger MHWs near the equator during El Niño, and to the south, north and west during La Niña (Holbrook et al., 2019).

On average, there are 1–3 MHW events per year at any particular location across the TWCPO, with a tendency for more frequent MHWs slightly north of the equator (Fig. 3a). The largest SST anomalies occur along the equator, in a pattern that aligns with ENSO (Fig. 3b). Mean MHW intensities along the equator are ~ + 2.5 °C, diminishing to ~ + 1 °C only a few hundred kilometres to the north and south. South of 20°S, the mean MHW intensity is more uniform, at around +1.7 °C. The mean MHW duration across the region is reasonably uniform, typically ~10 days, again with the exception of the equatorial band associated with ENSO (Fig. 3c). Since the zonal band along the equator is effectively the centre-of-action for ENSO dynamics, the longer persistence of El Niño events on average compared with variations elsewhere influences the longer mean MHW duration here at ~30 days. The area-averaged annual statistics of MHWs in the region are similar to those seen across the world's oceans (Oliver et al., 2018; c.f. their Fig. 1a,d,g), of which ENSO also dominates the variability in MHWs interannually as a global-scale average.

3.2. Marine heatwave variability and trends

Trends in MHW frequency, intensity and duration since 1982 show interesting patterns across the TWCPO (Fig. 3d-f). MHW frequency has increased at a rate of approximately one additional MHW event per decade across most of the region – except in the equatorial Pacific region east of 180°, a region that impinges on the western Pacific Warm Pool edge and which is influenced by large ENSO-related temperature variations in the equatorial cold tongue region, where there has been a weak decreasing trend (Fig. 3d). Over much of the TWCPO, there is not a notable MHW intensity trend, again apart from in the cold tongue region where there has been a clear reduction in MHW intensity (Fig. 3e). To some extent, the weak decreasing frequency of MHWs near the equator

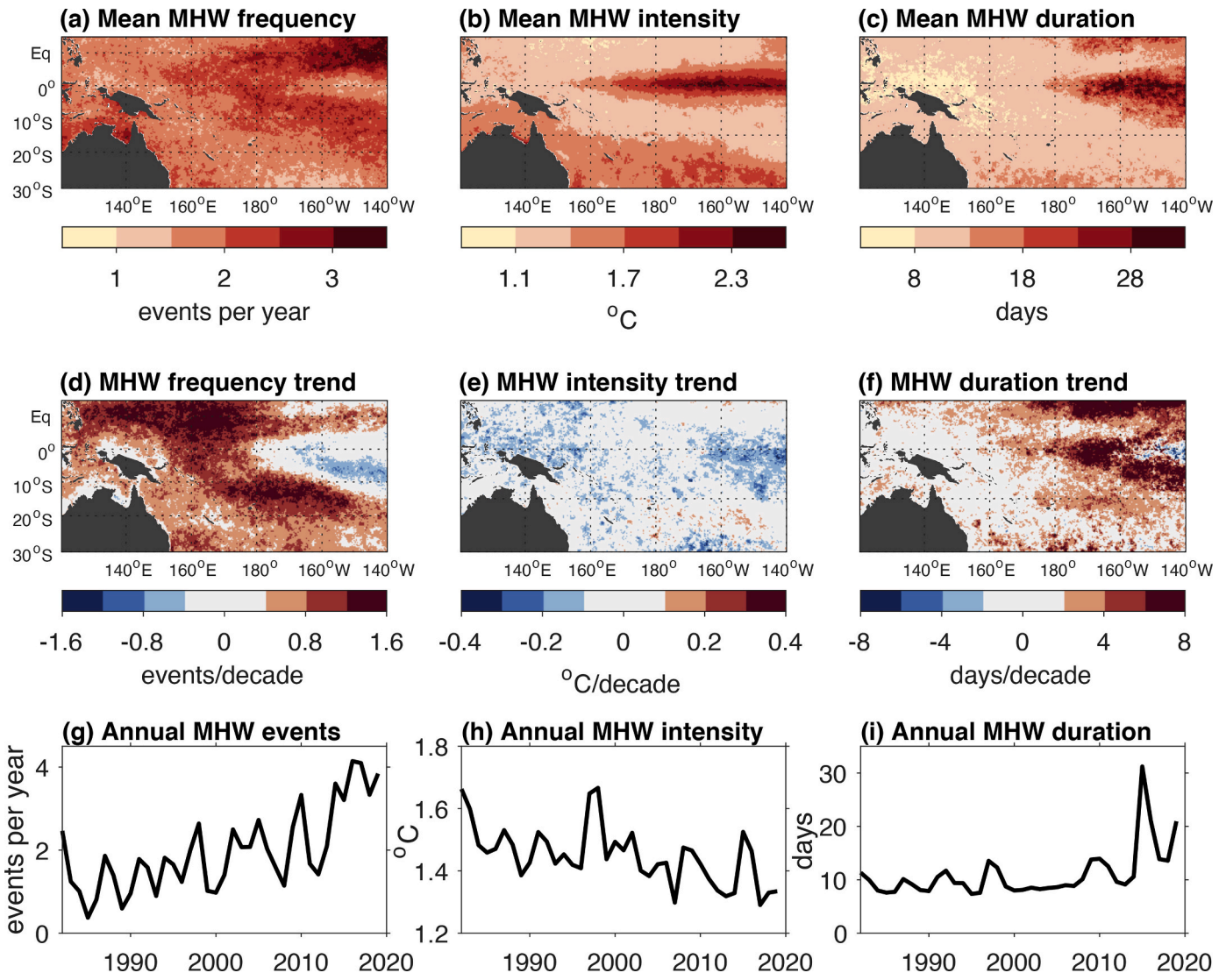

Fig. 3. Observed MHW statistics in the TWCPO. (a-c) Long-term means of annual mean statistics over the 1982–2019 period, where (a) frequency is the mean number of MHWs per year, (b) intensity is the annual mean of the maximum intensity of each MHW (as an anomaly in °C relative to the 1995–2014 climatology), and (c) duration is the annual mean duration of MHWs (in days). (d-f) Linear trends of the same statistics shown in (a-c) over the 1982–2019 period. (g-i) Annual time series of area averaged statistics over the TWCPO shown in (a-c).

can be explained by an increasing trend in MHW duration (Fig. 3f). MHWs in the eastern near equatorial and northeast parts of the domain have been increasing in duration at a rate of >4 days per decade. Across the rest of the region, there are no strong and consistent trends, but any that are apparent tend to be positive.

The timeseries of area averaged MHW statistics give a clearer picture of whole-of-region variations and trends over time. The overall increase in MHW frequency is clear (Fig. 3g), but there is a weak negative trend in MHW intensity (Fig. 3h) – noting that most of this trend is due to reduced intensities around the equator in the eastern portion of the TWCPO that is dominated by ENSO variations on SST. In terms of variability, the MHW duration timeseries is most notably marked by peaks corresponding to the extreme El Niño events of 1997/98 and 2015/16 and the strong Central Pacific El Niño of 2009/10 (Fig. 3i), which are also evident in the intensity timeseries (Fig. 3h). Interestingly for frequency, the trend is as large as the variability (Fig. 3g). These regional-scale characteristics are masked at the global-scale, where increasing trends in MHW frequency, intensity, and duration are observed in global-average timeseries (Oliver et al., 2018; c.f. their Fig. 1c,f,i). We expect that the absence of increasing trends across all MHW metrics in this region is largely due to the length of the record (only 38 years) that is dominated by the interdecadal variability in the Pacific. Specifically, the first 10–15 years of the 21st century was marked by a substantial negative Interdecadal Pacific Oscillation (IPO) phase, which caused cooler-than-usual SSTs across much of the tropical Pacific (e.g. England et al., 2014). Conversely, the latter part of the 20th century since 1976/77 was in the positive phase of the IPO. Hence, the Pacific has undergone transition from warm to cool phase generating a pattern of change across the Pacific consistent with the IPO (and/or Pacific Decadal Oscillation; PDO) signature in SST (e.g. Mantua et al., 1997; Power et al., 1999; Oliver et al., 2018; Holbrook et al., 2019).

Another important measure of MHWs is their category of intensity (Hobday et al., 2018). Here we present the mean numbers of days per year spent in categories from I-IV (i.e. categories otherwise named as Moderate, Strong, Severe, or Extreme), in two 20-year periods (Fig. 4). While again acknowledging the aforementioned transition from positive to negative phase of the IPO over the study period, and hence the potential role of this multi-decadal SST trend signature associated with the IPO across the region, it is clear that the mean number of Moderate MHW days per year increased from the period 1982–2001 to the period

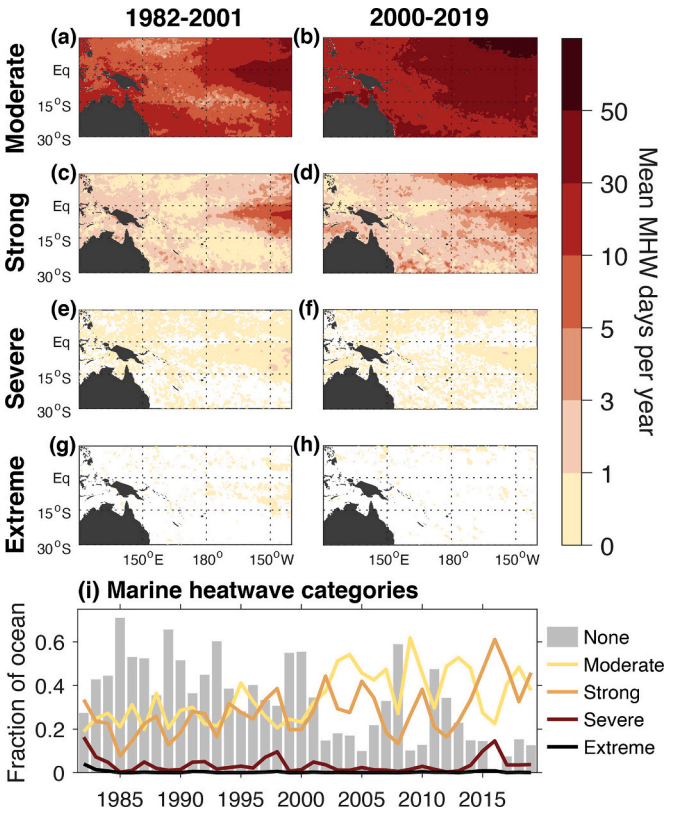

Fig. 4. Observed counts of MHW days in each category of intensity. (a-h) Mean MHW days per year over two over-lapping 20-year periods, following the MHW categorisation scheme of Hobday et al. (2018). Note that here the counts of Moderate MHW days include the numbers of days spent in any higher MHW category. (i) Maximum MHW category recorded, per year, over the fraction of ocean area depicted in (a-h).

2000–2019 (c.f. Fig. 4a and b). In the more recent period, there were at least 10 Moderate MHW days per year on average across the whole region, with most experiencing >30 days per year of MHW conditions (Fig. 4b). In contrast, some parts experienced fewer than 5 Moderate MHW days per year in the earlier period (Fig. 4a). So too have the number of Strong MHW days per year increased (Fig. 4c,d). However, any changes for Severe and Extreme MHW days are less clear, since MHWs with those intensities have been rare when considered against the 20-year baseline period of 1995–2014, even in the most recent years (Fig. 4e-h). Nevertheless, the timeseries of TWCPO area averaged MHW trends in Moderate and Strong category MHW days are clearly increasing, and the fraction of ocean not experiencing a MHW is decreasing (Fig. 4i). This is largely in agreement with the global picture (Hobday et al., 2018; their Fig. 5a).

4. Impacts of MHWs on three Pacific Island countries

In the following three subsections, we examine several key MHW events that have been observed over the study period and impacts experienced by the three Pacific Island countries (PICs) of Fiji, Samoa and Palau.

4.1. Fiji

Fiji is an archipelago of more than 300 islands in the southwest Pacific Ocean (17.7144°S, 178.0650°E), with the two largest islands of Viti

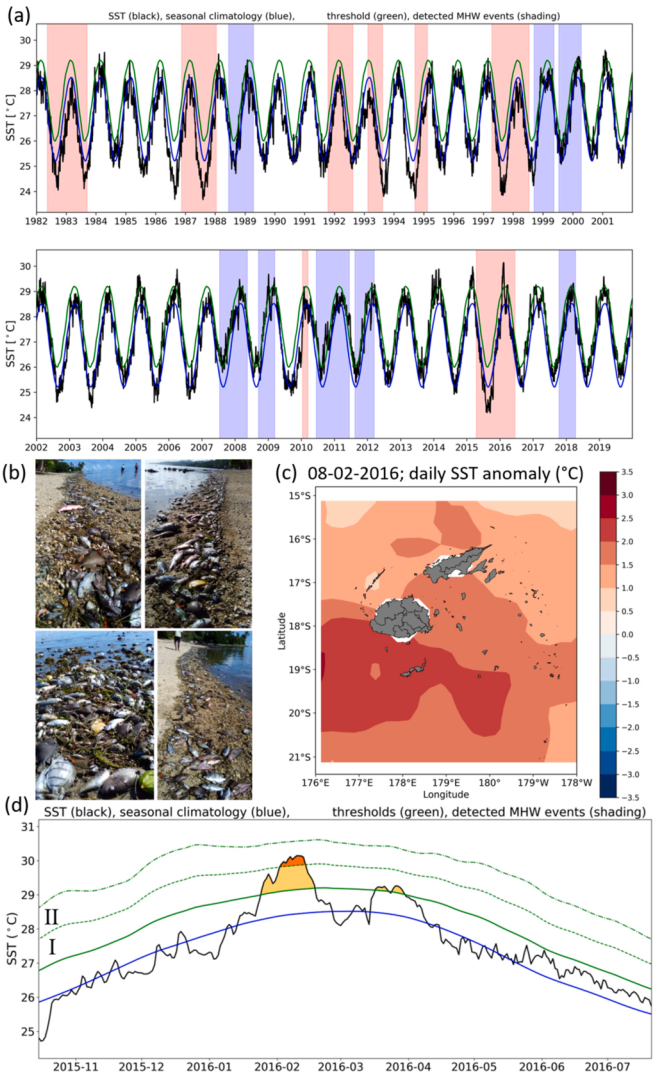

Fig. 5. (a) SST (°C) timeseries from 1982 to 2019 for the Fiji region showing the observed SST from OISST v2–1 (black line), the seasonal climatology (blue line; based on 30-year baseline, 1986–2015), and the 90th percentile threshold (green line). Pink and blue bars denote strong El Niño and La Niña events respectively. (b) Dead/dying fish and invertebrates washed up on beaches near Votua Village along Fiji's Coral Coast on Monday 8th February 2016 coinciding with elevated SSTs in the Fiji region. Photo source: Reef Explorer Fiji. (c) SST (°C) anomaly on 8th February 2016. (d) Area-averaged SST timeseries of the February 2016 event for the domain shown in (c), showing observed SST (black line), seasonal climatology (blue line), 90th percentile threshold (green solid line), 2× threshold (dashed line), and 3× threshold (dash-dot line). I: Category I "Moderate" MHW; II: Category II "Strong" MHW (following Hobday et al., 2018). (For interpretation of the references to colour in this figure legend, the reader is referred to the web version of this article.)

Levu, where the majority of the population resides, and Vanua Levu. Fiji's estimated population in 2017 was 884,887, with 56% living in urban areas (Fiji's Bureau of Statistics 2017[1]). The coastal region is vitally important, with most of the urban centres and vast majority of villages relying on ocean and coastal resources for food and livelihood, as well as commerce and its primary economies of agriculture and industry (primarily sugarcane production and processing) and tourism being located along the coast (Republic of Fiji, 2014).

Area-averaged SSTs for the Fiji region (Fig. 5a) indicate an increasing

[1] https://www.statsfiji.gov.fj/index.php

trend from 1982 to 2019, with the majority of the largest anomalously cool 'winters' occurring prior to the year 2000, and only two anomalously cool winters after 2006 – that is, in 2009, and in 2015 preceding the February 2016 MHW event. Overall, the warm seasons throughout much of the 1980s and 1990s were lower than the 30-year baseline average of these seasons (calculated from 1986 to 2015). Warmer-than-average and average years relative to baseline prevailed through the 2000s, and exceptionally warm years were experienced in 2014, 2015 and 2016. There does not appear to be a definitive ENSO signature on SSTs at this local country scale, but La Niña events tended to coincide with SSTs that were at, or above, the 90th percentile. In particular, while elevated SSTs were indeed observed during the extreme El Niño in 2015/16, relatively average SSTs were experienced in the Fiji region during the extreme El Niños of 1982/83 and 1997/98 (Fig. 5a).

A total of 82 MHW events occurred in the Fiji region in the period from 1982 to 2019. These were characterised by typical durations of ~5–40 days, but with three MHWs lasting more than 40 days in 2010 and 2011. The longest duration MHW was 61 days (26/05/2011–25/07/2011) with an average intensity of 1.27 °C above climatology, and an area-averaged maximum intensity of 1.92 °C above climatology. This event also ranked highest by cumulative intensity (77.28 °C days) and was ranked third in terms of maximum intensity.

Over the full timeseries, MHW area-averaged maximum intensities were typically 1–1.75 °C above the climatological mean, but there were two events exceeding +2.0 °C in 2010 and 2014. The most intense MHW event occurred in September/October 2010 with an area-averaged maximum intensity of 2.19 °C above climatology, and with some individual regions reaching much higher values. For example, a small region to the southeast of Viti Levu reached a maximum intensity of 3.96 °C above climatology. This event lasted for 42 days (12/09/2010–23/10/2010), with a cumulative intensity of 63.61 °C days. Whilst this event ranked highest in terms of maximum intensity, it ranked third in terms of duration and second by cumulative intensity.

The MHW events in 2010, 2011, 2014, 2015, and 2016 were all categorised as Strong (Category II) events at their peak. The February/March 2016 MHW had serious impacts for Fiji and over a broader reach (extending to Vanuatu and Kiribati), and was associated with the deaths of hundreds of marine fin fish and invertebrates including sea snakes, octopus, and crabs, which were found washed ashore on beach shorelines and floating on shallow reefs and waters (Fig. 5b). In Fiji, these were found in the Votua Village waters and beach along the Coral Coast in Viti Levu (pers. comm. Nanise Kuridrani, Fiji). In Vanuatu, dead fish were found floating in the Pango Village waters of the Emten Lagoon in Port Vila and Aneityum Island, while in Kiribati, large numbers of dead fish were found on Christmas Island (Kiritimati) beachfront and shorelines. These incidences were reported widely in local news.[2] The February 2016 MHW was a Strong category event for almost half (46%) of its duration (Fig. 5d) and reached an area-averaged maximum intensity of 1.70 °C above climatology, with individual areas experiencing much greater values. For example, on 8th February (when the photos of the dead/dying fish and invertebrates were taken), an anomalously warm region was evident to the southwest of Fiji with intensity 2.8 °C higher than climatology (Fig. 5c,d), and with anomalies of +3.1 °C experienced in eastern reefs by 15th February.

The 2016 MHW event was also associated with coral bleaching, which occurred after shallow reef areas along Fiji's Coral Coast had already experienced two back-to-back years of widespread coral bleaching.[3] The February 2016 surface (upper ocean) warming around Fiji was facilitated by a period of low wave energy along Fiji's Coral Coast, which reduced mixing and reef flushing, and likely exacerbated the effects of warming sea temperatures on reefs and shallow lagoons. The COSPPac Ocean Portal (http://oceanportal.spc.int/portal/app.html#climate) indicated wave heights along Fiji's Coral Coast were < 0.5 m for at least a week in early February 2016, which is below the typical lowest wave height during calm periods of >0.5 m in February for that region (defined as 10% of the lowest wave heights calculated for each month separately using wave hindcast data from1979–2013; Bosserelle et al., 2015).

Another case when a MHW apparently affected fish health occurred in Fiji in February 2019, when dead and weak live fish were discovered at the Suva foreshore and shallow waters at Muanikau along the Queen Elizabeth Drive at low tide. The live fish were found floating and gasping for air and could not swim.[4] The SST timeseries indicates that 2019 was an anomalously warm year (Fig. 5a).

Ocean temperature extremes (such as MHW events) can result in fish and invertebrate deaths when elevated seawater temperatures exceed species thermal tolerances, especially for those species that reside in or enter shallow waters and/or at low tides. In these environments, elevated SSTs can also be associated with reduced levels of dissolved oxygen in the seawater, contributing to animal stress and mortality (Roberts et al., 2019). MHWs can also exacerbate risks from harmful algal blooms, which have been associated with numerous fish kills worldwide (Roberts et al., 2019).

4.2. Samoa

Samoa is located in the southwest Pacific (13.7590°S, 172.1046°W) and has two large main islands, Savai'i and Upolu, that account for 99% of the total land area, surrounded by eight islets. These two main islands also account for 99% of Samoa's 195,979 population (Samoa Bureau of Statistics, 2017). The capital, Apia, is located on Upolu, the most populous and developed of the islands. Agriculture and fisheries are Samoa's primary industries, followed by manufacturing, construction, and tourism (Samoa, 2019). The reef area of Samoa is about 402 sq. km (Chin et al., 2011).

Area-averaged SSTs for the Samoa region (Fig. 6a) indicate a strong overall warming trend from 1982 to 2019, with most years experiencing below- to well-below-average cool season temperatures prior to 2004, and very few after 2004. An exception is the low cool season temperatures experienced in 2015 ahead of the elevated SSTs in 2016. Following the warm years in 1982–1984, there were nine consecutive years of warm season SSTs that remained under the extreme warm-water threshold and at times fell below climatology. This was in turn followed by a mix of average to above-average warm years in the 2000s and 2010s, culminating in five out of the last six years experiencing elevated SSTs (Fig. 6a). Many of the anomalously warm years coincided with strong or extreme El Niño events (e.g., 1983, 1998, 2010, and 2016), with many below-threshold years coinciding with La Niña events (e.g., 1989, 2000, 2008, 2011, 2012, and 2018). However, for the moderate El Niño years of 1987 and 1992, SSTs were not anomalously warm within the Samoa region.

A total of 89 MHW events occurred in the Samoa region over the period 1982–2019. These MHWs were characterised by durations of <20 days prior to 2004, with durations of ≥40 days more prevalent after 2005, with the two longest duration events of ~120 days occurring in the last four years (2016 and 2019). The 2019 MHW event had the longest duration of 124 days (from 17/05/2019–17/09/2019), with a cumulative intensity of 121.09 °C days, an average intensity of 0.98 °C above climatology, and a maximum intensity of 1.47 °C above

[2] https://www.spc.int/updates/news/2016/02/concern-over-dead-fish-fiji-and-vanuatu; https://asiapacificreport.nz/2016/02/09/vanuatu-heat-wave-suspected-cause-for-sudden-death-of-fish/; https://dailypost.vu/news/low-oxygen-in-water-kill-fish-says-fisheries/article_3e057e95-e37d-5d52-a47f-23e697a6e8ed.html; www.pina.com.fj/?p=pacnews&m82956c27787c5238ab096e3

[3] https://mission-blue.org/2016/08/coral-reef-recovery-in-fiji/

[4] https://www.pressreader.com/fiji/fiji-sun/20190214/282432760418104

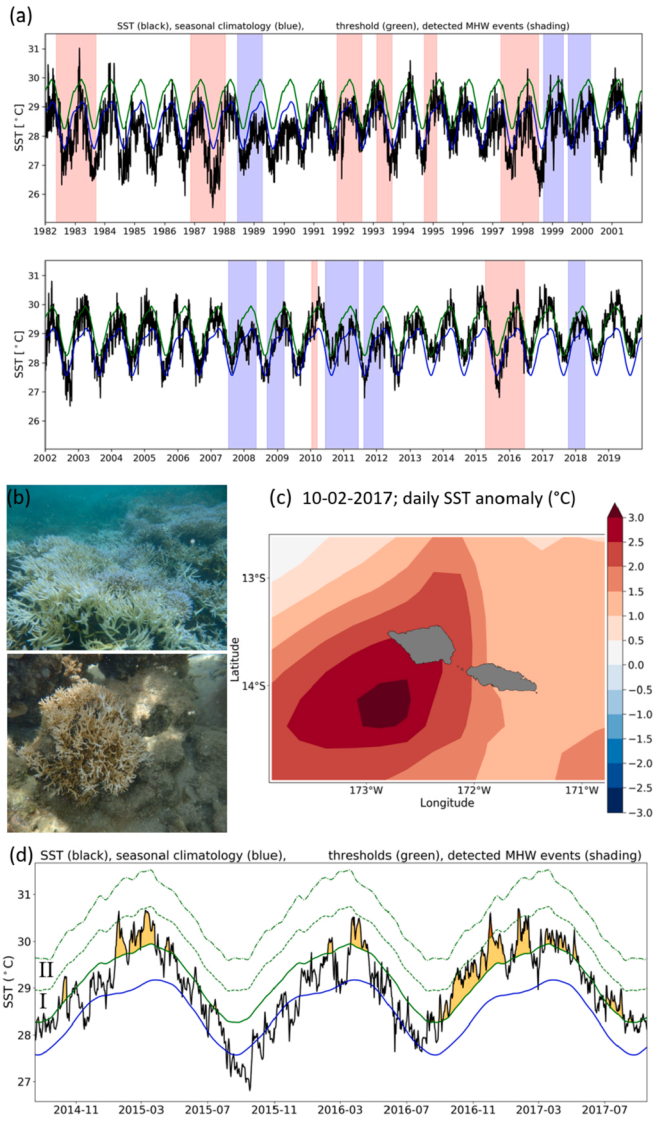

Fig. 6. (a) SST (°C) timeseries from 1982 to 2019 for the Samoa region showing observed SST (OISST v2–1; black line), seasonal climatology (blue line; based on 30-year baseline, 1986–2015), and the 90th percentile threshold (green line). Pink and blue bars denote strong El Niño and La Niña events respectively. (b) Bleached corals at (top) Satuiatua in 2015 (source: Satoa et al., 2016) and (bottom) Palolo Deep in 2017 (source: Roberta Mura-Faasavalu, Faculty of Science, National University of Samoa). (c) Anomalous SST during the 2017 MHW event, with maximum intensity of 3.11 °C above the climatological mean to the southwest. (d) Area-averaged SST timeseries from 2015 to 2017 for the domain shown in (c), showing observed SST (black line), seasonal climatology (blue line), 90th percentile threshold (green solid line), 2× threshold (dashed line), and 3× threshold (dash-dot line). I: Category I "Moderate" MHW; II: Category II "Strong" MHW (following Hobday et al., 2018). (For interpretation of the references to colour in this figure legend, the reader is referred to the web version of this article.)

climatology. This event was ranked 13th by maximum intensity, and second by cumulative intensity. The event was separated from an earlier MHW by only five days, during which time the temperature dropped 0.28 °C below the 90th percentile threshold. Had the two MHWs been counted as one, it would have lasted for 173 days.

Over the full timeseries, MHW maximum intensities were typically 1–1.75 °C above climatology, but with four MHWs exceeding +1.75 °C intensities occurring in 1983 and from 2015 to 2017. The most intense MHW occurred in February 1983 and had an area-averaged maximum intensity of 2.00 °C above the climatological mean, with some individual areas reaching 3.39 °C above the mean. This event was a Category II "Strong" event but lasted for only 6 days (from 22/02/1983–27/02/1983) and had a cumulative intensity of 10.67 °C days, with an average intensity of 1.78 °C above climatology. While this event ranked 1st (highest) in terms of maximum intensity, it only ranked 59th in terms of duration and 27th by cumulative intensity.

The MHW with the highest cumulative intensity (127.74 °C days) occurred over 114 days (from 07/09/2016–29/12/2016) with an area-averaged maximum intensity of +1.87 °C and an average intensity of +1.12 °C. This event was ranked second in terms of both duration and maximum intensity.

In the coral bleaching years of 2015 and 2017, individual regions within the Samoa region experienced elevated SSTs of 2.40 °C and 3.11 °C above the climatological mean in 2015 and 2017 respectively. At their peak, MHWs in both years reached Category II "Strong" (Fig. 6d). MHW events associated with coral bleaching events in 1998 and 2003 were Category I "Moderate" events (area-averaged over the Samoa region).

Major coral bleaching events were recorded in Samoa in 1997/98 and 2002/03 (Satoa et al., 2016), and between 2014 and 2017 (Ziegler et al., 2018). Bleaching events were reported around the country, including Satuiatua reef in Savaii and within the Palolo Deep Marine Reserve, located on the ocean side of the Apia Harbour region (Fig. 6b). Several reef surveys were conducted, and all showed high levels of bleaching and coral mortality. These included surveys conducted at several sites on Upolu in 2005 (Iakopo et al., 2005) and Savai'i in 2015 (Satoa et al., 2016) that found bleaching levels at some sites as high as 22% and 90% respectively. A study on the outer slope of a reef on the north coast of Upolu island in 2015 found 100% mortality in live coral (Berthe et al., 2016), which coincided with an unusually high temperature trend during January–May 2015 (evident in Fig. 6d). Surveys conducted in 2016 at 124 sites on coral reefs over 83 km of coastline at the island of Upolu found extremely low (<1%) coral cover at approximately half of the sites and < 10% coral cover at 78% of sites (Ziegler et al., 2018). The very poor and degraded states of the reefs were thought to be due not only to bleaching but also interaction with other stressors including crown-of-thorns outbreaks and anthropogenic activities (Ziegler et al., 2018).

4.3. Palau

The Republic of Palau is situated in the far western tropical northwest Pacific Ocean (7.5150°N, 134.5825°E). The archipelago comprises 586 islands, but only 12 are inhabited, and the majority of Palau's ~ 18,000 population live on the islands of Koror and Babeldaob (Republic of Palau, 2013). Palau is well-known internationally for its diverse natural ecosystems, with over 500 km^2 of coral reefs (Golbuu et al., 2007) and tourism is very important to Palau's economy.

Area-averaged SSTs for the Palau region (Fig. 7a) indicate an apparent general reduction in the seasonal SST range from 1982 to 2019, which is particularly apparent after 2008 while many years prior to 2008 experienced relatively cool winters (i.e., observed SSTs well below the seasonal climatology; Fig. 7a). The highest SSTs were recorded in 1998, in the transition from the extreme 1997/98 El Niño to La Niña, with other anomalously warm years coinciding with the 2010/11 La Niña period and the extreme El Niño in 2016 (2015/16). Anomalously warm years were also evident in 2017 and 2018, the latter following a La Niña event.

A total of 91 MHW events occurred in the Palau region over the period 1982–2019. These were characterised by typical durations of ~5–40 days, with several longer duration MHW events occurring in 1998 (70 days), 2010 (75 days), and 2018 (80 days). The longest MHW was 80 days (from 10/01/2018–30/03/2018) with a cumulative intensity of 79.27 °C days, an average intensity of 1.00 °C above climatology, and a maximum intensity of 1.48 °C above climatology. This event was ranked 12th by maximum intensity and third by cumulative

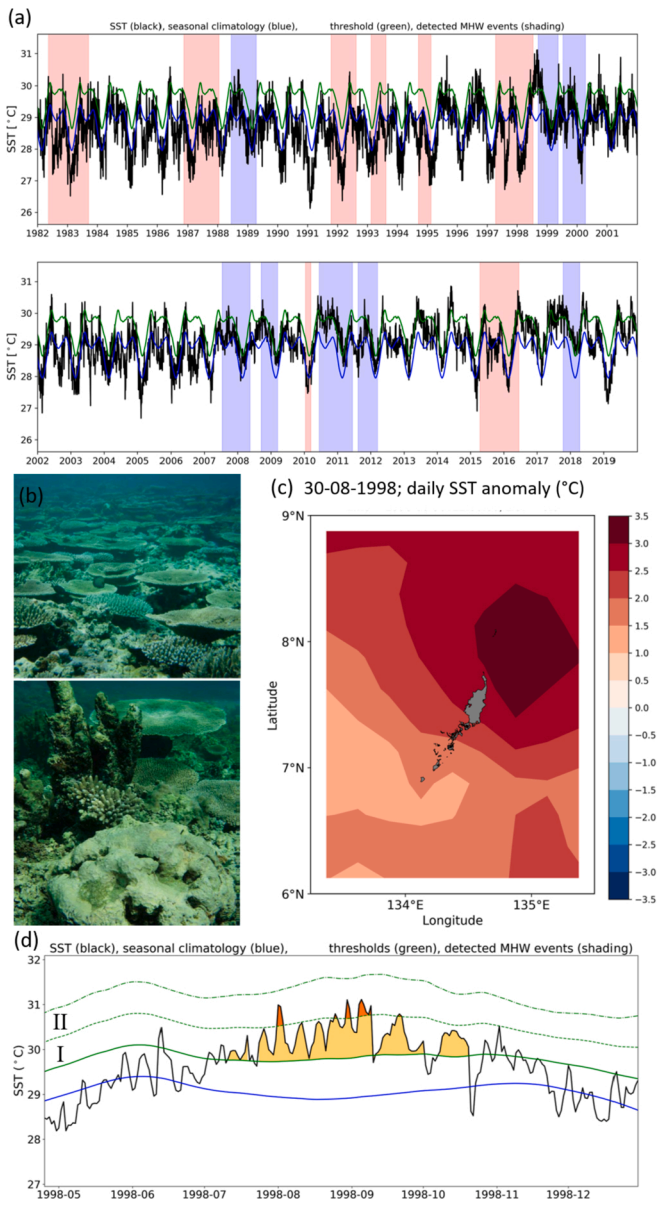

Fig. 7. (a) SST (°C) timeseries from 1982 to 2019 for the Palau region showing observed SST (OISST v2–1; black line), seasonal climatology (blue line; based on 30-year baseline, 1986–2015), and the 90th percentile threshold (green line). Pink and blue bars denote strong El Niño and La Niña events respectively. (b) *Acropora* dominance on northern patch reefs (June 2005) (top) and large dead colonies of *Psammocora digitata* (bottom photo; background left) and *Goniastrea edwardsi* (foreground). Source: Golbuu et al. (2007). [Fig. 7b images reprinted by permission from Springer Nature: *Coral Reefs* "Palau's coral reefs show differential habitat recovery following the 1998-bleaching event", (Golbuu et al., 2007)] (c) Anomalous SST during the 1998 MHW event, with maximum intensity of 3.49 °C above climatology to the northeast. (d) Area-averaged SST timeseries of the 1998 event for the Palau region in (c), showing observed SST (black line), seasonal climatology (blue line), 90th percentile threshold (green solid line), 2× threshold (dashed line), and 3× threshold (dash-dot line). I: Category I "Moderate" MHW; II: Category II "Strong" MHW (following Hobday et al., 2018). (For interpretation of the references to colour in this figure legend, the reader is referred to the web version of this article.)

intensity.

Over the full timeseries, MHW maximum intensities were typically 1.0–1.5 °C above the climatological mean, but there were nine events with maximum intensities > + 1.5 °C. The most intense MHW event occurred in 1998 and had an area-averaged maximum intensity of 2.19 °C above climatology, with individual regions experiencing anomalous SSTs of +3.49 °C (Fig. 7c). This event had an average intensity of 1.43 °C above climatology and lasted for 70 days (from 24/07/1998–01/10/1998), with a cumulative intensity of 99.85 °C days. While this event ranked first (highest) in terms of maximum and cumulative intensity, it ranked third in terms of duration and second by mean intensity.

The 1998 MHW event reached Category II "Strong" intensity on four occasions, spanning 24% of the MHW event's duration, and otherwise often remained close to the Category II limit (Fig. 7d). Elevated SSTs in 2010 and 2017 were Category I "Moderate" MHW events for much of their duration but reached Category II "Strong" at their peaks.

Coral bleaching occurred in Palau in 1998 and 2010. Bruno et al. (2001) quantified the extent of the coral bleaching caused by the elevated SSTs in 1998 in Palau, and found widespread bleaching at numerous sites across the main islands of Palau, with total bleaching mortality of nearly 48% of coral colonies belonging to 20 scleractinian taxa, while partial bleaching affected 15% of all colonies surveyed. Golbuu et al. (2007) assessed the recovery rates of coral communities in Palau based on data from 2001 to 2005. Coral coverage was dominated by *Acropora* plates with a conspicuous absence of large massive colonies (Fig. 7b). Palau's sheltered bay reefs were the least impacted from the 1998 thermal stress event. However, outer exposed reefs experienced high coral mortality. In 2010, western Micronesia experienced a regional thermal stress event, resulting in severe bleaching in Palau's northwestern lagoon on the outer barrier and patch reefs (van Woesik et al., 2012). The earliest bleaching was recorded in late June 2010, and by mid-July bleaching was observed in most reef habitats (van Woesik et al., 2012). Our analysis indicates that SSTs remained anomalously warm for much of the latter half of 2010 and into early 2011 (Fig. 7a).

Despite elevated SSTs in 2014, 2016, and 2017, Palau only experienced mass coral bleaching events in 1998 and 2010. There has been very little bleaching between 2010 and the present day in Palau, at least not on a scale for bleaching surveys (Koshiba, 2020). Examination of the area-averaged SST data indicates that while SSTs were higher in 2014 than 2010, they occurred over a shorter duration than in 2010.

5. Future projections of MHWs

5.1. CMIP6 multi-model mean evaluation

Individual CMIP6 models vary in their simulations of MHW characteristics and patterns. However, the multi-model mean can be used as a guide to more accurately estimate MHW characteristics when compared to observations, and to help assess the confidence that can be placed in future projections. We assess model performance by comparing the simulated MHW characteristics in the CMIP6 *historical* simulations to those from the observed OISST v2–1 data (Fig. 8). The most notable bias appears in the simulation of Moderate category MHW days for the period 2000–2019. The multi-model mean overestimates the number of MHW days per year by more than 20 days in some parts of the TWCPO (Fig. 8j). The mean number of Strong, Severe, and Extreme MHW days per year also tends to be overestimated by up to 5 days (Fig. 8l,n,p). These differences are most likely largely due to the background interdecadal variability signature in the observations that are not well represented in the models. As noted earlier, the study period spans the change from a positive to strong negative IPO phase, the timing of which is not necessarily expected in the coupled and "free running" CMIP6 models. In the earlier period (1982–2001), the mean model bias is much weaker, and the largest signals emerge mainly due to pattern differences between the observed data and the model mean field, in which the variations among individual simulations are smoothed out.

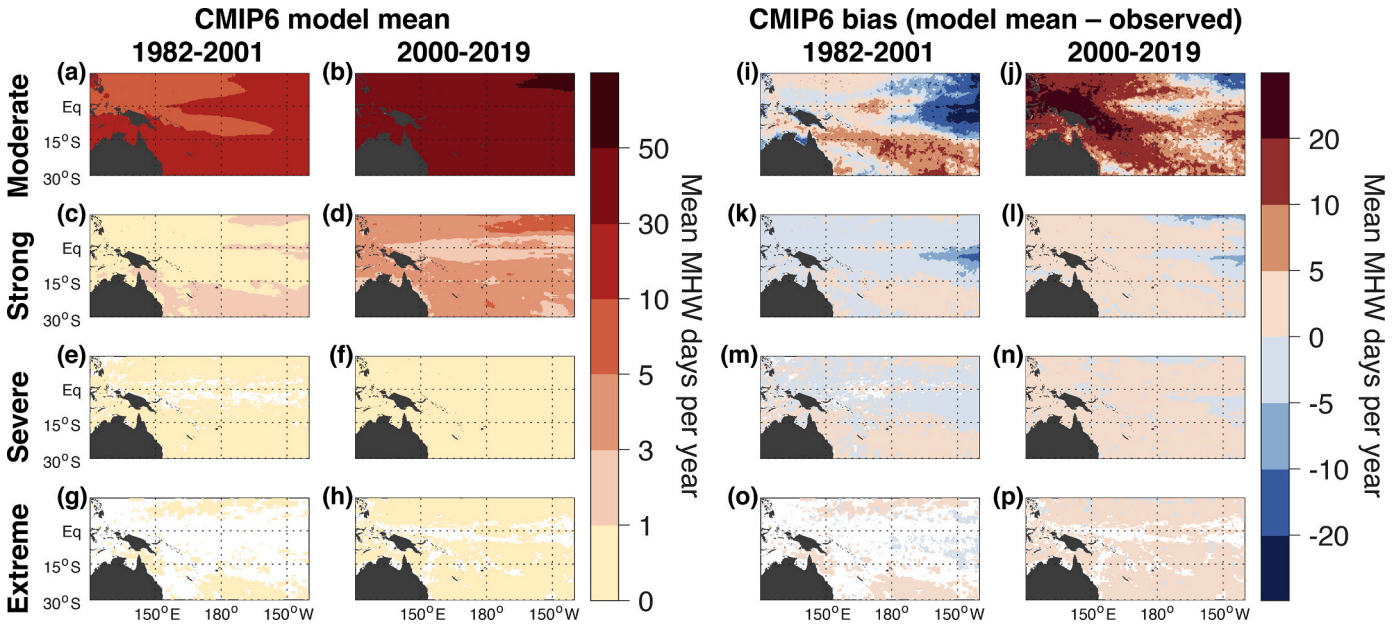

Fig. 8. Multi-model mean (MMM) CMIP6 *historical* simulations of the mean number of MHW days per year in each category of intensity. (a-h) Mean MHW days per year over two overlapping 20-year periods, as in Fig. 4a-h. (i-p) CMIP6 model mean bias, represented as the difference between the MMM MHW estimates and observations in Fig. 4a-h.

5.2. CMIP6 projections of MHWs in the TWCPO

The CMIP6 projections show vastly different possible outcomes over the next few decades for the TWCPO, depending upon future global greenhouse gas emissions scenarios. Two possible future shared socio-economic pathway (SSP) scenarios from the Scenario Model Intercomparison Project (ScenarioMIP; O'Neill et al., 2016) were analysed here: a low emissions scenario, (i.e. SSP1–2.6), and a high emissions scenario (i.e. SSP5–8.5). Note here that projected numbers of MHW days per year are based on current day baselines (here, 1995–2014), and do not account for shifting baselines as the planet warms.

The projected numbers of MHW days per year for each MHW intensity category (I-IV) are shown for two 20-year periods under the SSP1–2.6 and SSP5–8.5 scenarios (Fig. 9). Both scenarios lead to more projected MHW days per year (dpy) by the year 2050, but to vastly differing degrees. The differences between the scenarios for the earlier period (2020–2039) are negligible (c.f. Fig. 9a,c,e,g and 9i,k,m,o). However, there is a strong divergence in the two outcomes for the later period (2040–2059). Under the low emissions scenario, the multi-model mean projects more than 100 Moderate intensity MHW dpy across the

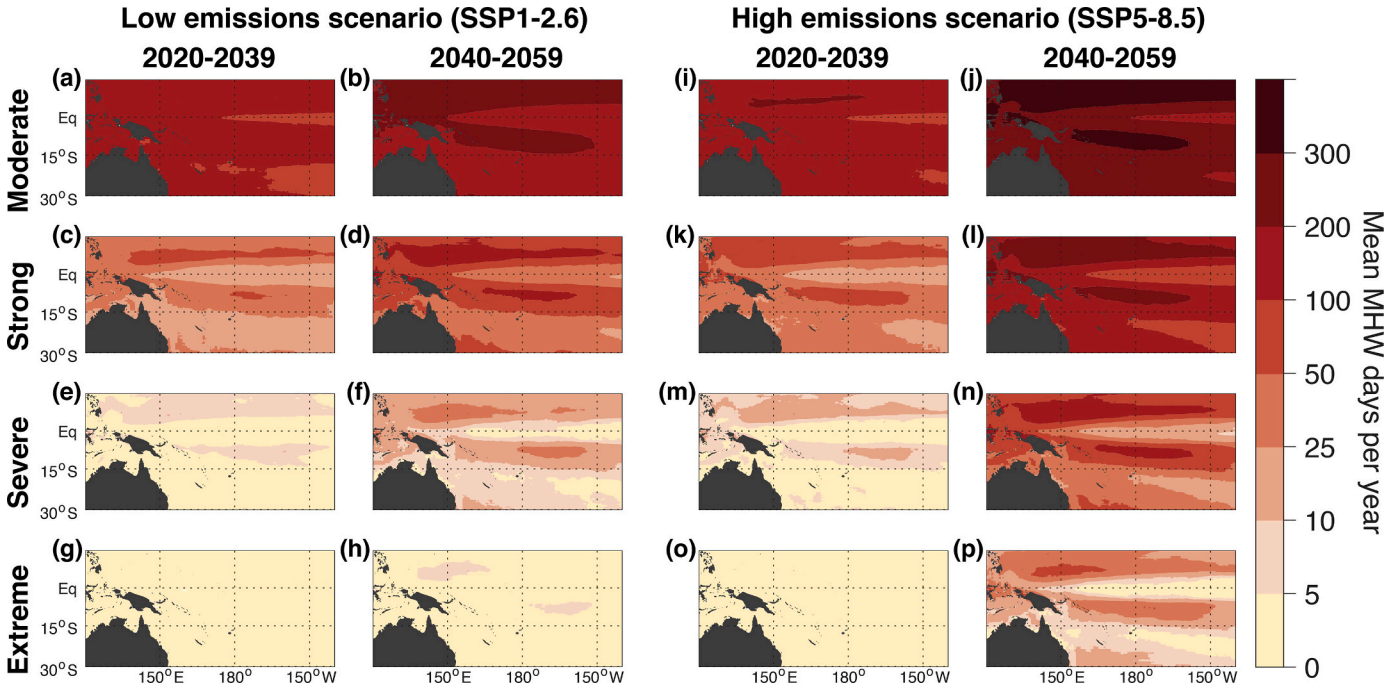

Fig. 9. CMIP6 multi-model mean average number of MHW days per year in each intensity category under the two future greenhouse gas emissions scenarios. (a-h) Mean MHW days per year in the SSP1–2.6 scenario over two future 20-year periods, as in Fig. 8a-h. (i-p) As in (a-h), but for the SSP5–8.5 scenario.

region, and more than 200 dpy in the Moderate category nearer the equator (Fig. 9b). This is in contrast to the 10–50 Moderate MHW dpy experienced today (Fig. 4b). For the high emissions scenario, a minimum of 200 Moderate MHW dpy are projected by 2050, with more than 300 dpy nearer the equator (Fig. 9j). Notably more MHW dpy are projected under SSP5–8.5 across each of the MHW categories for the later period (2040–2059), as compared with SSP1–2.6 (c.f. Fig. 9d,f,h and 9l,n,p). The starkest contrast is in the projected number of Extreme MHW dpy. What is a relatively rare occurrence under today's climate (<1 day per year), more than 50 dpy are projected to experience Extreme MHW conditions in some areas by 2050 under the high emissions scenario (Fig. 9p). Under the low emissions scenario, Extreme MHWs are likely to occur fewer than 5 dpy (Fig. 9h).

5.3. CMIP6 projections of MHWs for Fiji, Samoa and Palau

The area-averaged timeseries of annual number of MHW dpy by intensity category show similar characteristics for Fiji, Samoa, and Palau (Fig. 10). Note that the domains here are slightly different to those shown in Fig. 1 and analysed in Section 4. The domains are given in the Fig. 10 caption. Each PIC region is projected to experience a near-constant Moderate, and likely even Strong, MHW category state by the end of the 21st century under the high (SSP5–8.5) emissions scenario (as indicated by the red multi-model mean line approaching 365 days per year; Fig. 10a-f). Under the low (SSP1–2.6) emissions scenario, the number of Moderate and Strong MHW days per year are also substantially elevated in the latter half of the 21st century, but to a lesser degree (blue multi-model mean line; Fig. 10a-f). The starkest difference between the two scenarios is again most apparent for the Extreme MHW category: that is, over half of the year in the multi-model mean under the SSP5–8.5 scenario, but still close to zero in the multi-model mean under the SSP1–2.6 scenario (Fig. 10j-l).

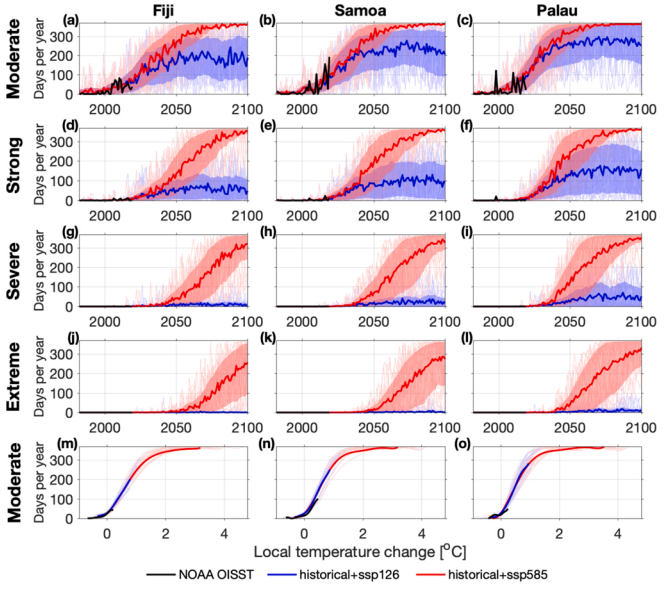

Fig. 10. Annual MHW days in each intensity category under the two future greenhouse gas emissions scenarios (low emissions, SSP1–2.6, and high emissions, SSP5–8.5). SST data were area-averaged for each region before computing the marine heatwave statistics. (a,d,g,j,m) Fiji: 174°E-178°W, 21–14°S. (b,e,h,k,n) Samoa: 174–170°W, 15–12°S. (c,f,i,l,o) Palau: 130–136°E, 2–9°N. (m,n,o) Relationship between the local annual mean SST (averaged over the aforementioned areas for each region, respectively) and the number of annual Moderate MHW days. The mean SST and annual MHW day timeseries were first smoothed with a 10-year running mean, and the lines shown are 7th order polynomial fits to the smoothed data. In each panel, individual models are plotted as thin lines, model means as thick coloured lines, and OISST denoted by thick black lines. On panels (a-l), red and blue shading denotes the *likely* model range, representing the central 66% of models. The *likely* ranges have been smoothed with a 10-year running mean. (For interpretation of the references to colour in this figure legend, the reader is referred to the web version of this article.)

Though the projections largely display similar characteristics in the MHW-category timeseries across the three PICs, there are nevertheless some interesting points of difference. Fiji, for example, exhibits a marginally slower growth across all MHW categories under both scenarios. Although there is substantial model spread in these results, no single model projects that there will be zero Moderate intensity MHW days per year in Samoa or Palau beyond 2050, under either emissions scenario (Fig. 10b,c).

There is a strong relationship between the local mean SST change and expected marine heatwave days (Fig. 10m,n,o). Changes to SST variability or skewness may alter the relationship, but there is little spread among the models. To provide more complete information that should be of value to marine managers of fisheries and biodiversity, we include an additional row of panels in Fig. 10 (m,n,o) quantifying the important functional relationship between the number of Moderate marine heatwave days and local average temperature change. We note here that differences in the curves across the three regions are relatively minor. Because there is such a strong relationship between mean temperature change and marine heatwave characteristics, as measures of ocean temperature extremes (as outlined by Oliver (2019)), this connection has utility for estimating scenario-independent projections of marine heatwave days based on the expected temperature change alone.

6. Discussion

6.1. Impact implications for Pacific Island Countries and Territories

Marine heatwaves (MHWs) in the tropical western and central Pacific Ocean region (TWCPO) have increased in frequency and duration over the last 40 years and have led to tangible impacts such as fish and invertebrate mortality, and coral bleaching in and around, for example, Vanuatu, Kiribati, Fiji, Palau, and Samoa. For the latter three Pacific Island countries, reported in the present paper, these impacts were associated with MHWs that were Category II ("Strong") events at their peak. Historical gridded sea surface temperature observations (daily OISST from 2000 to 2019) indicate that, on average, Fiji, Samoa, and Palau experience 1–3 Strong category MHW days per year. However, under the low emissions scenario (SSP1–2.6), the model-mean climate change projections indicate that by 2050 there may be ~50 Strong MHW days per year on average for Fiji, and ~ 100 Strong MHW days per year on average for Samoa and Palau. Under the high emissions scenario (SSP5–8.5), these values increase to ~100 Strong MHW days by 2050 for Fiji, and ~ 200 Strong MHW days for Samoa and Palau (Fig. 10; but noting that there is a wide range in the projected MHW days across models). Furthermore, Category IV ("Extreme") MHWs are projected to increase from an average of <1 day per year in the present climate to >25 days per year on average by 2050 in regions near Palau, and >50 days per year in some Pacific regions.

It is important to note that CMIP6 models exhibit a wider range in climate sensitivity than CMIP5 (Zelinka et al., 2020), which may translate to a wider range in the marine heatwave metrics analysed here. There is some indication that the CMIP6 range might be reduced by weighting models based on performance and independence (Brunner et al., 2020), and future work on marine heatwave projections might follow such an approach.

Given the impact that Strong MHW events have apparently already had in the Pacific, the projected increases in the number of Strong MHWs and higher incidences of Severe and Extreme events in the future will almost certainly have serious implications for the food security, livelihoods, and health of communities in Pacific Island countries. Consumption rates of fresh fish among Pacific coastal communities are

among the highest in the world, with the average consumption in many Pacific Island Countries and Territories (PICTs) being 2–4 times the global average – with fish comprising 50–90% of the animal protein consumed in coastal rural areas, and much of it coming from coastal demersal species (Bell et al., 2009; Dunstan et al., 2018). Household surveys conducted in Samoa in 2009 on the purpose of fishing indicated that home consumption (subsistence fishing) was the main reason (65%), followed by mixed consumption and sales (32%), and just 3% for pure sales (Tiitii et al., 2014). Most of this effort was directed at inshore fishing (72%), with just 9% offshore, and 18% both inshore and offshore (Tiitii et al., 2014). Coastal fisheries in the Pacific often provide an income for local communities, with an average of 50% of surveyed coastal households in 17 PICTs indicating that they receive their first or second income from fishing-related activities (Pinca et al., 2010; Dunstan et al., 2018). Furthermore, ecotourism is a popular income-generating activity for many local communities, which could potentially be negatively impacted from the degradation of coral reefs through more frequent and/or prolonged MHW events in the future that allow less time for recovery between events, and exacerbated by other extreme events where a larger proportion of the reef may bleach. All of these changes have the potential to impact cultural dimensions, with cultural significance associated with many natural places, marine species, and practices (Johnson et al., 2020).

Changes to coastal fisheries under climate change are particularly worrying in the context of projections for reduced catch potential in tropical oceans in the future, suggesting that the potential to supplement diet and income through offshore fisheries may also be reduced. There is high confidence that ocean warming and changes in primary productivity in the 21st century will reduce the global maximum catch potential, with some areas including the western central Pacific experiencing $\geq$3 times the decrease in catch potential than the global average by 2100 under the high emissions scenario RCP8.5 (IPCC, 2019). In terms of reef-based fisheries, Bell et al. (2013) organised 22 PICTs into three groups based on the area of coral reef available per person to produce fish, with one group (which included Fiji and Samoa) with the lowest ratio of coral reef habitat per capita already experiencing a wide gap between the sustainable harvests of demersal fish available from coral reefs and the recommended fish consumption of 35 kg per person per year. It was suggested that this gap will be expected to increase significantly due to population growth and climate change.

MHWs also have health implications for Pacific nations. Increases in SST can promote the growth of harmful algae blooms (HABs; Frölicher and Laufkötter, 2018; Roberts et al., 2019), which have had negative impacts on the food security, tourism, local economy, and human health of Pacific Island countries and their communities (IPCC, 2019). HABs contain organisms (usually algae) that cause various negative impacts when they bloom, including fish kills, environmental degradation due to high biomass, and various forms of human illnesses such as eating fish contaminated with ciguatoxin (Ralston and Moore, 2020). Ciguatera poisoning in humans is characterised by gastrointestinal, neurological and cardiovascular disturbances, and cases of severe toxicity can result in paralysis, coma and death (Lehane and Lewis, 2000). There is no immunity, and symptoms may persist for months or years, or recur periodically (Lehane and Lewis, 2000). The primary source of ciguatoxin that causes ciguatera fish poisoning is the benthic dinoflagellates *Gambierdiscus spp*. (Erdner et al., 2008), which are found in tropical and subtropical coral reef ecosystems in association with various macroalgae. Their distribution and growth appear to be influenced by abrupt (e.g., hurricanes, storms, heavy rains) or gradual (increasing sea surface temperature (SST), salinity, and nutrient concentrations) stressor changes on their natural environment (Chateau-Degat et al., 2005). However, increased SST is commonly suggested as the most important factor that enhances toxic algal blooms and ciguatoxin production (Yang et al., 2016). Projected increases in MHWs in the Pacific region increase ciguatera-risk with regards to incidence and areas affected. In Fiji, reported incidences of ciguatera fish poisoning over a period of 10 years (2008–2017) increased by 207% from 854 cases in 2008 to 1775 in 2017, with a total incidence of 15,114 cases reported. An incidence of fish poisoning occurred in 2016/17 in Gau island, in Fiji's Lomaiviti archipelago, where 13 people were poisoned after eating Bluestripe herring (*Herklotsichthys quadrimaculatus*) of which four people died.[5] The highest incidence occurred in 2012 in which 2000 cases were reported (Nand, 2017). These figures may not fully represent the real situation, as it appears that fish poisoning incidences in Fiji (and possibly elsewhere in the Pacific) are under-reported because: (1) only serious cases visit hospitals and health centres, while mild cases are usually not reported because they do not visit hospitals and often do not seek medical attention, particularly in locations where syndromic management is well known to the community in the prevalent use of herbal traditional medicine, and (2) in rural communities, long distances with poor road conditions to the hospital or health centre prevent people from easily visiting and seeking medical assistance. With the projected increases in MHWs in the future, further investigation is warranted into the future risk associated with the distribution of toxic dinoflagellate *Gambierdiscus* and the incidence of ciguatera fish poisoning.

An important consideration for marine heatwave projections and their impacts in future is the potential for ecological adaptation. With a shifting baseline under global warming, some species may find it possible to adapt better than others, or there may be a restructuring of the ecosystem (Smale et al., 2019). The fixed baseline approach adopted here is somewhat inflexible to the potential for adaptability. An alternative view of marine heatwaves is to quantify 'thermal displacement', or the distance required to move to inhabit the same level of climatological temperature (Jacox et al., 2020). Such a measure of marine heatwaves is applicable to mobile marine species, but less relevant to immobile or benthic entities, including coral.

6.2. Potential predictability and the need for prediction

Being able to predict MHW events at various lead times could provide tangible benefits to Pacific island local communities, resource managers, and aquaculture enterprises (Dunstan et al., 2018; Holbrook et al., 2020b). At short forecast lead times, predictability would facilitate raising awareness to avoid health implications of eating dead/decaying fish and the risk of ciguatera poisoning, and enabling agencies to consider temporarily increasing access to other fish sources (e.g., nearshore pelagics; Dunstan et al., 2018). A range of short-term techniques to protect corals from bleaching are currently being tested on Pacific reefs (e.g., shading of corals, Coelho et al., 2017) and these could potentially be deployed ahead of a predicted MHW event. Similarly, aquaculture facilities could also benefit from advanced notice of a MHW event, providing time to implement both short- and long-term measures such as lowering oyster lines to deeper cooler water, cooling incoming seawater into onshore aquaculture facilities, or moving stock to less heat-susceptible areas. Ocean and climate forecasts, that are shown to be potentially skilful on subseasonal-to-seasonal timescales, may be beneficial to provide information on the likelihood or probability of a MHW event in the weeks to months ahead. Salinger et al. (2016), White et al. (2017), Dunstan et al. (2018) and Holbrook et al. (2020b) provide comprehensive reviews and perspectives on the forecasting benefits and challenges, and note that end-users should understand that forecasts will not always be accurate, but that sustained use should lead to more positive outcomes in the long term.

On longer timescales (1–10 years), potentially skilful prediction systems would enable fishery and coastal managers, businesses, and communities to make strategic, policy, and investment decisions (Salinger et al., 2016). At these timescales, predictability largely relies on understanding the connection between MHWs and large-scale climate

[5] https://www.fijitimes.com.fj/fish-poisoning-kills-4/

drivers, such as ENSO, the Southern Annular Mode (SAM) and the Interdecadal Pacific Oscillation (IPO), as well as local modifying processes (e.g., circulation patterns, mesoscale eddies, local processes that modulate local air-sea heat fluxes). For the TWCPO, there are genuine opportunities going forward to take advantage of climate prediction systems being developed that tap into the predictability of these modes of climate variability and their teleconnections. A recent global assessment of MHWs and their drivers (Holbrook et al., 2019) highlighted the connection to ENSO (tropical Pacific) and SAM (south-central and western Pacific regions), which is reinforced by MHW event analyses in those regions where persistent anticyclones associated with blocking of atmospheric flows and reduced wind speeds have been important contributors to MHW conditions (Lee et al., 2010; Salinger et al., 2019, 2020). For example, a strong 2009/10 MHW event in the south-central Pacific was associated with an extreme and persistent anticyclone which decreased wind speed and diverted circumpolar westerlies and warm air towards Antarctica, causing oceanic warming primarily through reduced latent and sensible (oceanic) heat loss and by weaker advection of cold waters from the south (Lee et al., 2010). Recent (2017/18 and 2019/20) MHWs in the New Zealand region were associated with a strong positive SAM, anomalously low winds and atmospheric circulation anomalies comprising a pattern of blocking to the east and southeast of New Zealand, with negative pressure anomalies to the northwest. The associated very low wind speeds and reduced upper ocean mixing allowed air-sea heat fluxes to cause substantial warming of the stratified surface layers of the Tasman Sea (Salinger et al., 2019, 2020). In the current study, the 2016 MHW event in Fiji was associated with low winds and wave energy along the Coral Coast, which reduced mixing and reef flushing, and likely exacerbated the effects of warming sea temperatures on the reefs and shallow lagoons. Further event-based analyses of atmospheric and oceanic drivers in the case study regions were beyond the scope of the present study.

6.3. Mitigation and adaptation

Given the observed and potential impacts from Strong or higher category MHW events, there is likely to be a time in the future when adaptation options and the utility of being able to predict MHW events may be insufficient to protect Pacific island communities from MHW impacts superimposed on a warming ocean. The emissions pathway that we ultimately take over the next couple of decades as a global society will play a large part in determining at what point in the future that occurs, or whether it occurs at all. Our study shows the substantial difference between the projected effects of choosing a high or low emissions scenario in the number and severity of MHW days per year in the decades ahead. Under the high emissions scenario, each region is projected to experience a near-constant Moderate, and likely even Strong, MHW category state by the year 2100. By contrast, this is substantially reduced under the low emissions scenario. Similarly, under the high emissions scenario, and relative to the current baseline, the present-day equivalent of Extreme MHW conditions are projected for over half of the year by 2100, whereas Extreme MHW occurrences remain close to zero under the low emissions scenario.

Data availability statement

Observational NOAA 0.25° daily Optimum Interpolation Sea Surface Temperature (OISST), version 2.1 metadata and access are available at https://doi.org/10.25921/RE9P-PT57. CMIP6 data can be searched for and accessed at the Earth System Grid Federation portal at https://esgf.nci.org.au/search/cmip6-nci. The processed marine heatwave data for observations and CMIP6 shown in Sections 3 and 5 are described in Kajtar et al. (2021), and available for download at https://doi.org/10.5281/zenodo.5069012. The code for processing the observational and CMIP6 data is available at https://github.com/jbkajtar/mhw_pacific. Marine heatwave metrics were computed using the marineHeatWaves python module, which is available at https://github.com/ecjoliver/marineHeatWaves. Subsurface temperature data were made available through the ReefTEMPS project via their website http://www.reeftemps.science/en/data/.

Declaration of Competing Interest

The authors declare that they have no known competing financial interests or personal relationships that could have appeared to influence the work reported in this paper.

Acknowledgments

We would like to gratefully acknowledge and thank the Secretariat of the Pacific Regional Environment Programme (SPREP) for hosting the two important workshops from 23-26 September 2019 and 28-31 October 2019 in Apia, Samoa, that facilitated the initial design and development of this paper. In particular, we would like to sincerely thank Azarel Mariner (SPREP) and Geoff Gooley (CSIRO Oceans and Atmosphere) for co-convening these workshops. We would like to gratefully acknowledge the participants in attendance who contributed to group discussions including Morgan Wairiu and (Robert) Duncan McIntosh. We gratefully acknowledge funding provided by the Australian Government-funded (Australia-Pacific Climate Partnership) Next-Gen Projections for the Western Tropical Pacific project, led by CSIRO in partnership with SPREP, that enabled workshop participants to travel from various Pacific countries to Samoa, to be accommodated, fed and looked after for these workshops. We acknowledge the World Climate Research Programme's Working Group on Coupled Modelling, which is responsible for CMIP, and we thank the climate modelling groups for producing and making available their model output. CMIP6 model outputs were made available with the assistance of resources from the National Computational Infrastructure (NCI), which is supported by the Australian Government. We thank NOAA and ReefTEMPS for making their data publicly available. NJH and JBK acknowledge ongoing support from the Australian Research Council (ARC) Centre of Excellence for Climate Extremes (CE170100023) and the National Environmental Science Programme Earth Systems and Climate Change Hub (Project 5.8). We acknowledge Eric Oliver for the use of his marineHeatWaves python module. We also acknowledge the assistance of Paola Petrelli in the ARC Centre of Excellence for Climate Extremes for her computational support and assistance with data archiving. Finally, we would like to thank the three anonymous reviewers whose comments helped to improve the manuscript.

References

Arafeh-Dalmau, N., Schoeman, D.S., Montaño-Moctezuma, G., et al., 2020. Marine heat waves threaten kelp forests. Science (80) 367, 635.

Arias-Ortiz, A., Serrano, O., Masqué, P., et al., 2018. A marine heatwave drives massive losses from the world's largest seagrass carbon stocks. Nat. Clim. Chang. 8, 338–344.

Ballester, J., Giorgi, F., Rodó, X., 2009. Changes in European temperature extremes can be predicted from changes in PDF central statistics. Clim. Chang. 98, 277–284.

Bell, J.D., Kronen, M., Vunisea, A., et al., 2009. Planning the use of fish for food security in the Pacific. Mar. Policy 33, 64–76.

Bell, J.D., Reid, C., Batty, M.J., et al., 2013. Effects of climate change on oceanic fisheries in the tropical Pacific: Implications for economic development and food security. Clim. Chang. 119, 199–212.

Berthe, C., Chancerelle, Y., Lecchini, D., Hedouin, L., 2016. First report of a dramatic rapid loss of living coral on the north coast of western Samoa. Vie Milieu 66, 155–157.

Bosserelle, C., Reddy, S., Lal, D., 2015. WACOP Wave Climate Reports. Fiji nearshore Wave Hindcast. Secretariat of the Pacific Community, Votua Passage. http://gsd.spc.int/wacop/.

Brunner, L., Pendergrass, A.G., Lehner, F., et al., 2020. Reduced global warming from CMIP6 projections when weighting models by performance and independence. Earth Syst. Dyn. 11, 995–1012.

Bruno, J., Siddon, C., Witman, J., et al., 2001. El Niño related coral bleaching in Palau, Western Caroline Islands. Coral Reefs 20, 127–136.

Caputi, N., Kangas, M., Denham, A., et al., 2016. Management adaptation of invertebrate fisheries to an extreme marine heat wave event at a global warming hot spot. Ecol. Evol. 6, 3583–3593.

Caputi, N., Kangas, M., Chandrapavan, A., et al., 2019. Factors affecting the recovery of invertebrate stocks from the 2011 Western Australian extreme marine heatwave. Front. Mar. Sci. 6, 484.
Chateau-Degat, M.L., Chinain, M., Cerf, N., et al., 2005. Seawater temperature, Gambierdiscus spp. variability and incidence of ciguatera poisoning in French Polynesia. Harmful Algae 4, 1053–1062.
Cheung, W.W.L., Frölicher, T.L., 2020. Marine heatwaves exacerbate climate change impacts for fisheries in the Northeast Pacific. Sci. Rep. 10, 6678.
Chin, A., Lison De Loma, T., Reytar, K., et al., 2011. Status of coral reefs of the Pacific and outlook: 2011. Global Coral Reef Monitoring Network, 260 p. https://researchonline.jcu.edu.au/24292/2/24292_Chin_et_al_2011_front_pgs.pdf.
Coelho, V.R., Fenner, D., Caruso, C., et al., 2017. Shading as a mitigation tool for coral bleaching in three common Indo-Pacific species. J. Exp. Mar. Biol. Ecol. https://doi.org/10.1016/j.jembe.2017.09.016.
Di Lorenzo, E., Mantua, N., 2016. Multi-year persistence of the 2014/15 North Pacific marine heatwave. Nat. Clim. Chang. 6, 1042–1047.
Dunstan, P.K., Moore, B.R., Bell, J.D., et al., 2018. How can climate predictions improve sustainability of coastal fisheries in Pacific Small-Island developing States? Mar. Policy 88, 295–302.
England, M.H., McGregor, S., Spence, P., et al., 2014. Recent intensification of wind-driven circulation in the Pacific and the ongoing warming hiatus. Nat. Clim. Chang. 4, 222–227.
Erdner, D.L., Dyble, J., Parsons, M.L., et al., 2008. Centers for oceans and human health: a unified approach to the challenge of harmful algal blooms. Environ. Heal A Glob. Access Sci. Source 7, S2.
Fiedler, T., Pitman, A.J., Mackenzie, K., et al., 2021. Business risk and the emergence of climate analytics. Nat. Clim. Chang. https://doi.org/10.1038/s41558-020-00984-6.
Frölicher, T.L., Laufkötter, C., 2018. Emerging risks from marine heat waves. Nat. Commun. 9, 650.
Frölicher, T.L., Fischer, E.M., Gruber, N., 2018. Marine heatwaves under global warming. Nature 560, 360–364.
Giorgi, F., Gutowski Jr., W.J., 2015. Regional dynamical downscaling and the CORDEX initiative. Annu. Rev. Environ. Resour. 40, 467–490.
Golbuu, Y., Victor, S., Penland, L., et al., 2007. Palau's coral reefs show differential habitat recovery following the 1998-bleaching event. Coral Reefs 26, 319–322.
Grose, M.R., Narsey, S., Delage, F.P., et al., 2020. Insights from CMIP6 for Australia's future climate. Earth's Futur. 8 e2019EF001469.
Hales, S., Weinstein, P., Woodward, A., 1999. Ciguatera (fish poisoning), El Niño, and Pacific Sea surface temperatures. Ecosyst. Health 5, 20–25.
Hewitson, B.C., Daron, J., Crane, R.G., et al., 2014. Interrogating empirical-statistical downscaling. Clim. Chang. 122, 539–554.
Hobday, A.J., Alexander, L.V., Perkins-Kirkpatrick, S.E., et al., 2016. A hierarchical approach to defining marine heatwaves. Prog. Oceanogr. 141, 227–238.
Hobday, A.J., Oliver, E.C.J., Sen Gupta, A., et al., 2018. Categorizing and naming marine heatwaves. Oceanography 31, 162–173.
Holbrook, N.J., Scannell, H.A., Sen Gupta, A., et al., 2019. A global assessment of marine heatwaves and their drivers. Nat. Commun. 10, 2624.
Holbrook, N.J., Sen Gupta, A., ECJ, Oliver, et al., 2020b. Keeping pace with marine heatwaves. Nat. Rev. Earth Environ. https://doi.org/10.1038/s43017-020-0068-4.
Holbrook, N.J., Claar, D.C., Hobday, A.J., et al., 2020a. ENSO-driven ocean extremes and their ecosystem impacts. In: MJ, McPhaden, Santoso, A., Cai, W. (Eds.), El Niño Southern Oscillation in a Changing Climate. American Geophysical Union (AGU), pp. 409–428.
Huang, B., Liu, C., Banzon, V., et al., 2021. Improvements of the Daily Optimum Sea Surface Temperature (DOISST) - Version 2.1. J. Clim. 34, 2923–2939.
Hughes, T.P., Anderson, K.D., Connolly, S.R., et al., 2018a. Spatial and temporal patterns of mass bleaching of corals in the Anthropocene. Science (80) 359, 80–83.
Hughes, T.P., Kerry, J.T., Baird, A.H., et al., 2018b. Global warming transforms coral reef assemblages. Nature 556, 492–496.
Iakopo, M., Ward, J., Ifopo, P., et al., 2005. Coral Bleaching Assessment Report – Safata Marine Protected Area 2005. Apia, Samoa.
IPCC, 2019. IPCC Special Report on the Ocean and Cryosphere in a Changing Climate. https://www.ipcc.ch/srocc/.
Jacox, M.G., Alexander, M.A., Bograd, S.J., Scott, J.D., 2020. Thermal displacement by marine heatwaves. Nature 584, 82–86.
Johnson, J., Bertram, I., Chin, A., et al., 2018. Effects of climate change on fish and shellfish relevant to Pacific Islands, and the coastal fisheries they support. Pacific Marine Clim. Change Report Card: Sci. Rev. 74–98.
Johnson, J.E., Allain, V., Basel, B., et al., 2020. Impacts of Climate Change on Marine Resources in the Pacific Island Region. In: Climate Change and Impacts in the Pacific. Springer, pp. 359–402.
Kajtar, J.B., Hernaman, V., Holbrook, N.J., Petrelli, P., 2021. Tropical western and central Pacific marine heatwave data calculated from gridded sea surface temperature observations and CMIP6. Data Br. submitted.
Koshiba, S., 2020. Palau International Coral Reef Center, Personal Communication.
Lee, T., Hobbs, W.R., Willis, J.K., et al., 2010. Record warming in the South Pacific and western Antarctica associated with the strong central-Pacific El Niño in 2009-10. Geophys. Res. Lett. 37, L19704.
Lehane, L., Lewis, R.J., 2000. Ciguatera: recent advances but the risk remains. Int. J. Food Microbiol. 61, 91–125.
Li, L., Hollowed, A.B., Cokelet, E.D., et al., 2019. Subregional differences in groundfish distributional responses to anomalous ocean bottom temperatures in the northeast Pacific. Glob. Chang. Biol. https://doi.org/10.1111/gcb.14676.
Llewellyn, L.E., 2010. Revisiting the association between sea surface temperature and the epidemiology of fish poisoning in the South Pacific: Reassessing the link between ciguatera and climate change. Toxicon 56, 691–697.
Mantua, N.J., Hare, S.R., Zhang, Y., et al., 1997. A Pacific interdecadal climate oscillation with I. Bull. Am. Meterol. Soc. 78, 1069–1080.
McPhaden, M.J., Zebiak, S.E., Glantz, M.H., 2006. ENSO as an integrating concept in earth science. Science (80) 314, 1740–1745.
McPhaden, M.J., Santoso, A., Cai, W., 2020. El Niño Southern Oscillation in a Changing Climate. American Geophysical Union (AGU). Geophysical Monograph Series.
Mills, K.E., Pershing, A.J., Brown, C.J., et al., 2013. Fisheries management in a changing climate: lessons from the 2012 ocean heat wave in the Northwest Atlantic. Oceanography 26, 191–195.
Nand, D., 2017. Fish Poisoning 1995–2017. Suva, Fiji. (pers. comm.).
Nurse, L.A., McLean, R.F., Agard, J., et al., 2014. Small Islands. Cambridge University Press.
Oliver, E.C.J., 2019. Mean warming not variability drives marine heatwave trends. Clim. Dyn. 53, 1653–1659.
Oliver, E.C.J., Wotherspoon, S.J., Holbrook, N.J., 2014. Estimating extremes from global ocean and climate models: a Bayesian hierarchical model approach. Prog. Oceanogr. 122, 77–91.
Oliver, E.C.J., Benthuysen, J.A., Bindoff, N.L., et al., 2017. The unprecedented 2015/16 Tasman Sea marine heatwave. Nat. Commun. 8, 1038.
Oliver, E.C.J., Donat, M.G., Burrows, M.T., et al., 2018. Longer and more frequent marine heatwaves over the past century. Nat. Commun. 9, 1324.
Oliver, E.C.J., Burrows, M.T., Donat, M.G., et al., 2019. Projected Marine heatwaves in the 21st century and the potential for ecological impact. Front. Mar. Sci. 6, 734.
O'Neill, B.C., Tebaldi, C., Van Vuuren, D.P., et al., 2016. The Scenario Model Intercomparison Project (ScenarioMIP) for CMIP6. Geosci. Model Dev. 9, 3461–3482.
Pearce, A., Lenanton, R., Jackson, G., et al., 2011. The "marine heat wave" off Western Australia during the summer of 2010/11. Fisheries Research Report No. 222. Department of Fisheries, Western Australia, p. 40. http://fish.wa.gov.au/Documents/research_reports/frr222.pdf.
Pearce, A.F., Feng, M., 2013. The rise and fall of the "marine heat wave" off Western Australia during the summer of 2010/2011. J. Mar. Syst. 111–112, 139–156.
Pershing, A.J., Mills, K.E., Dayton, A.M., et al., 2018. Evidence for adaptation from the 2016 marine heatwave in the Northwest Atlantic Ocean. Oceanography. https://doi.org/10.5670/oceanog.2018.213.
Pinca, S., Kronen, M., Friedman, K., et al., 2010. Regional Assessment Report: Profiles and Results from Survey Work at 63 Sites Across 17 Pacific Island Countries and Territories. Pacific Regional Oceanic and Coastal Fisheries Development Programme (PROCFish/C/CoFish), Noumea, New Caledonia.
Power, S.B., Casey, T., Folland, C.K., et al., 1999. Inter-decadal modulation of the impact of ENSO on Australia. Clim. Dyn. 15, 319–324.
Ralston, D.K., Moore, S.K., 2020. Modeling harmful algal blooms in a changing climate. Harmful Algae 91, 101729.
Republic of Fiji, 2014. Second National Communication to the United Nations Framework Convention on Climate Change. Suva, Fiji: Ministry of Foreign Affairs, 130 pp, ISBN 978-982-9163-01-1, https://unfccc.int/resource/docs/natc/fjinc2.pdf.
Republic of Palau, 2013. Second National Communication to the United Nations Framework Convention on Climate Change. September 2013, https://www4.unfccc.int/sites/SubmissionsStaging/NationalReports/Documents/45823961_Palau-NC2-1-Final_Palau%20National%20Communication.pdf.
Reynolds, R.W., Smith, T.M., Liu, C., et al., 2007. Daily high-resolution-blended analyses for sea surface temperature. J. Clim. 20, 5473–5496.
Roberts, S.D., van Ruth, P., Wilkinson, C., et al., 2019. Marine heatwave, harmful algae blooms and an extensive fish kill event during 2013 in South Australia. Front. Mar. Sci. 6, 610.
Salinger, J., Hobday, A.J., Matear, R.J., et al., 2016. Decadal-scale forecasting of climate drivers for marine applications. Adv. Mar. Biol. 1–68.
Salinger, M.J., Renwick, J., Behrens, E., et al., 2019. The unprecedented coupled ocean-atmosphere summer heatwave in the New Zealand region 2017/18: Drivers, mechanisms and impacts. Environ. Res. Lett. 14, 044023.
Salinger, M.J., Diamond, H.J., Behrens, E., et al., 2020. Unparalleled coupled ocean-atmosphere summer heatwaves in the New Zealand region: drivers, mechanisms and impacts. Clim. Chang. 162, 485–506.
Samoa, 2019. Second National Communication to the United Nations Framework Convention on Climate Change. Samoa, p. 99. https://unfccc.int/resource/docs/natc/samnc2.pdf.
Samoa Bureau of Statistics, 2017. 2016 Census Brief No. 1. Revised version: Population Snapshot and Household Highlights. Samoa Bureau of Statistics, p. 66. https://www.sbs.gov.ws/digi/2016_Census_Brief_No.1.pdf.
Satoa, M., Kwan, S., Ward, J., Faitua, J., 2016. Assessment of The Mass Coral Bleaching in Samoa Due to Increase in Sea Surface Temperatures 2015. Marine Conservation Section, Division of Environment and Conservation, Ministry of Natural Resources and Environment, Apia, Samoa.
Scannell, H., Pershing, A., Alexander, M.A., et al., 2016. Frequency of marine heatwaves in the North Atlantic and North Pacific since 1950. Geophys. Res. Lett. 43, 2069–2076.
Simolo, C., Brunetti, M., Maugeri, M., Nanni, T., 2011. Evolution of extreme temperatures in a warming climate. Geophys. Res. Lett. 38, L16701.
Skinner, M.P., Brewer, T.D., Johnstone, R., et al., 2011. Ciguatera fish poisoning in the Pacific Islands (1998 to 2008). PLoS Negl. Trop. Dis. 5, e1416.
Smale, D.A., Wernberg, T., Oliver, E.C.J., et al., 2019. Marine heatwaves threaten global biodiversity and the provision of ecosystem services. Nat. Clim. Chang. 9, 306–312.
Straub, S.C., Wernberg, T., Thomsen, M.S., et al., 2019. Resistance, extinction, and everything in between – the diverse responses of seaweeds to Marine Heatwaves. Front. Mar. Sci. 6, 763.

The World Bank, 2013. Acting on Climate Change and Disaster Risk for the Pacific. The World Bank, p. 15. https://www.worldbank.org/content/dam/Worldbank/document/EAP/Pacific%20Islands/climate-change-pacific.pdf.

Tiitii, U., Sharp, M., Ah-Leong, J., 2014. Apia, Samoa Samoa Socioeconomic Fisheries Survey Report: 2012-2013. Secretariat of the Pacific Community (SPC), Noumea, New Caledonia, p. 52. https://spccfpstore1.blob.core.windows.net/digitallibrary-docs/files/eb/eb3f9535b37703fe92aad3a9537b85f3.pdf?sv=2015-12-11&sr=b&sig=J%2Btg501dlI07VjN8D8eo0jJVNRAaYWBroQy5jszPz5c%3D&se=2022-05-12T01%3A45%3A08Z&sp=r&rscc=public%2C%20max-age%3D864000%2C%20max-stale%3D86400&rsct=application%2Fpdf&rscd=inline%3B%20filename%3D%22Tiitii_14_Samoa_Socioeconomic.pdf.

Wernberg, T., Smale, D.A., Tuya, F., et al., 2013. An extreme climatic event alters marine ecosystem structure in a global biodiversity hotspot. Nat. Clim. Chang. 3, 78–82.

Varillon, D., Fiat, S., Magron, F., et al., 2021. ReefTEMPS: The Pacific Island Coastal Ocean Observation Network. SEANOE, https://doi.org/10.17882/55128.

Wernberg, T., Bennett, S., Babcock, R.C., et al., 2016. Climate-driven regime shift of a temperate marine ecosystem. Science (80) 353, 169–172.

White, C.J., Carlsen, H., Robertson, A.W., et al., 2017. Potential applications of subseasonal-to-seasonal (S2S) predictions. Meteorol. Appl. https://doi.org/10.1002/met.1654.

van Woesik, R., Houk, P., Isechal, A.L., et al., 2012. Climate-change refugia in the sheltered bays of Palau: Analogs of future reefs. Ecol. Evol. 2, 2474–2484.

World Health Organization, 2015. Human Health and Climate Change in Pacific Island Countries. World Health Organization Regional Office for the Western Pacific, p. 144. https://apps.who.int/iris/handle/10665/208253.

Yang, Q., Cokelet, E.D., Stabeno, P.J., et al., 2019. How "the Blob" affected groundfish distributions in the Gulf of Alaska. Fish. Oceanogr. 28, 434–453.

Yang, Z., Luo, Q., Liang, Y., Mazumder, A., 2016. Processes and pathways of ciguatoxin in aquatic food webs and fish poisoning of seafood consumers. Environ. Rev. 24, 144–150.

Zelinka, M.D., Myers, T.A., McCoy, D.T., et al., 2020. Causes of higher climate sensitivity in CMIP6 models. Geophys. Res. Lett. 47 e2019GL085782.

Zhang, L., Xu, Y., Meng, C., et al., 2020. Comparison of statistical and dynamic downscaling techniques in generating high-resolution temperatures in china from CMIP5 GCMs. J. Appl. Meteorol. Climatol. 59, 207–235.

Ziegler, M., Quéré, G., Ghiglione, J.F., et al., 2018. Status of coral reefs of Upolu (Independent State of Samoa) in the South West Pacific and recommendations to promote resilience and recovery of coastal ecosystems. Mar. Pollut. Bull. 129, 392–398.